NRC Research Press

ARTICLE

Climate-driven biophysical changes in feeding and breeding environments explain the decline of southernmost European Atlantic salmon populations

Ana Almodóvar, Daniel Ayllón, Graciela G. Nicola, Bror Jonsson, and Benigno Elvira

Abstract: The consistency of the global declining trend of Atlantic salmon (*Salmo salar*) populations suggests that climate-driven reduced survival and growth at sea are the main driving factors. The southernmost populations have experienced the greatest declines, consistent with harsher conditions in natal fresh waters. We analyzed temporal trends in Spanish Atlantic salmon, important food organisms at sea, and climatic variables in the breeding (fresh water) and feeding (marine) salmon areas from 1950 onwards to elucidate drivers of declining patterns. Salmon abundance dropped abruptly in 1970–1971, plausibly linked to widespread overfishing coincident with incipient changes in the marine food webs and freshwater hydrology. A major regime shift in biophysical conditions throughout the North Atlantic salmon feeding grounds occurred in 1986–1987, driven by the concurrence of an abrupt acceleration in the anthropogenic warming trend and the warm phase of the Atlantic Multidecadal Oscillation. This regime shift may be the proximate cause of the collapse of Spanish salmon observed in 1988–1989, which kept declining in parallel to trends of ever-increasing ocean and freshwater temperatures, decreasing river flows, and poorer marine trophic conditions.

Résumé : La cohérence de la tendance planétaire à la baisse des populations de saumon atlantique (*Salmo salar*) porte à croire que les réductions de la survie et de la croissance en mer causées par le climat en sont les principaux facteurs. Les populations les plus méridionales ont subi les plus grandes baisses, ce qui concorde avec des conditions plus difficiles dans les eaux douces natales. Nous avons analysé les tendances dans le temps du saumon atlantique espagnol, d'importants organismes lui servant de nourriture en mer et de variables climatiques dans ses aires de reproduction (en eau douce) et d'alimentation (en mer) à partir de 1950, afin de cerner les causes de ces déclins. L'abondance du saumon a chuté abruptement en 1970–1971, cette baisse étant plausiblement liée à la coïncidence d'une surpêche répandue et de modifications émergentes aux réseaux trophiques marins et à l'hydrologie des cours d'eau douce. Un important changement du régime de conditions biophysiques dans toutes les aires d'alimentation du saumon dans l'océan Atlantique Nord s'est produit en 1986–1987, causé par la cooccurrence d'une accélération soudaine du réchauffement d'origine anthropique et de la phase chaude de l'oscillation atlantique multidécennale. Ce changement de régime pourrait être la cause proximale de l'effondrement du saumon espagnol observé en 1988–1989, qui s'est poursuivi parallèlement à des tendances d'augmentation continue des températures de l'eau de mer et de l'eau douce, de diminution des débits des rivières et de détérioration des conditions trophiques marines. [Traduit par la Rédaction]

Introduction

Current climate change is a main driver of the biodiversity loss that will not only increase but also accelerate global and local extinctions (Urban 2015). Specifically, both marine and freshwater ectothermic organisms exhibit very high sensitivity to global warming, as their upper thermal tolerances typically correspond to the past temperatures experienced across their ranges (Sunday et al. 2012; Comte and Olden 2017*a*). Recent estimations indicate that in the last 50 years, over 20% of the global ocean may have undergone important species turnovers, and almost 30% may have experienced net quantitative biodiversity changes, the North Atlantic (NA) temperate biome being one of the hot spots (Beaugrand et al. 2015).

Atlantic salmon (*Salmo salar*) is an anadromous fish naturally distributed in European and North American rivers. Its marine feeding areas are in systems that have experienced recent climate-driven regime shifts, both in the Northeast Atlantic and its adjacent seas (e.g., Reid et al. 2001; Beaugrand et al. 2008; Hátún et al. 2009; Luczak et al. 2011), as well as in Northwest Atlantic ecosystems (e.g., Friedland and Todd 2012; Mills et al. 2013). In recent decades, the pre-fishery abundance (Chaput 2012; Friedland et al. 2014), reported fishery nominal catches (ICES 2018), and return rates of spawners (Friedland et al. 2009) have declined for the North American and European stock complexes, especially for the multi-sea-winter (MSW) salmon population in southern Europe (Beaugrand and Reid 2012; Friedland et al. 2014; Nicola et al. 2018). The lack of recovery in stock sizes despite substantial reductions in fishing pressure (total NA catches decreased from a mean value of 9934 t in 1960–1969 to 1877 t in 2008–2017; ICES 2018), together with the spatial coherence observed in the global declining trend, suggest that basin-scale climatic changes are involved (Beaugrand and Reid 2012; Mills et al. 2013; Friedland et al. 2014). Recruitment

Received 30 July 2018. Accepted 16 November 2018.

A. Almodóvar, D. Ayllón, and B. Elvira. Department of Biodiversity, Ecology and Evolution, Complutense University of Madrid (UCM), E-28040 Madrid, Spain.
G.G. Nicola. Department of Environmental Sciences, University of Castilla–La Mancha (UCLM), E-45071 Toledo, Spain.
B. Jonsson.* Landscape Ecology Department, Norwegian Institute for Nature Research, 0349 Oslo, Norway.
Corresponding author: Ana Almodóvar (email: aalmodovar@bio.ucm.es).
*Bror Jonsson currently serves as an Associate Editor; peer review and editorial decisions regarding this manuscript were handled by Keith Tierney.

of European salmon populations appears mainly driven by postsmolt survival during the first summer at sea (Friedland et al. 2009), which is growth-mediated through the functional relationship between the postsmolts and their predators (Jonsson and Jonsson 2009). Reduced sea growth resulting from the aforementioned climate-driven ecosystem shifts, with less productive pelagic food webs and increased competition from other zooplanktivore fishes, might be the underlying cause of declining salmon abundance (Jonsson et al. 2016).

The declining trend in Atlantic salmon abundance is most evident at the southern edge of the distribution range in Europe and North America (Jonsson and Jonsson 2009). The southernmost European populations are located in northern Spain. This geographical area was a refuge of Atlantic salmon during the Pleistocene glaciations (Consuegra et al. 2002; Finnegan et al. 2013). The remaining populations represent distinct evolutionary lineages and are thus an essential component of both the genetic diversity of the species and its evolutionary potential in the face of global change. Currently, these populations decline (Nicola et al. 2018) and change in genetic and life-history traits (Valiente et al. 2010, 2011; Horreo et al. 2011*a*), correlatively linked to local and large-scale climatic trends. However, the underlying causes of the decline in Spanish salmon are elusive, mostly because their spatial and temporal distributions in the ocean are practically unknown. Recent studies (e.g., MacKenzie et al. 2012) suggest that southern European one-sea-winter (1SW) salmon are likely to mix in a common feeding area comprising the southern Norwegian Sea, north of the Faroe Islands and south of Iceland. The European MSW salmon follow a different migratory route. Populations from the west coast of the UK and Ireland migrate more westerly towards West Greenland (MacKenzie et al. 2011, 2012; Olafsson et al. 2016), and the few available tag records suggest that Spanish salmon follow the same path (Jacobsen et al. 2012; Reddin et al. 2012). Thus, climatic and biological conditions in both the East and West NA probably influence Spanish populations.

Notwithstanding the pervasive role of marine survival, factors influencing survival, life history, and migration in fresh water have marked effects on salmon abundance dynamics (Otero et al. 2011). The vulnerability of freshwater fish to warming is expected to be greater in areas with higher predicted climatic exposure in the future (30°N–50°N; Comte and Olden 2017*b*). This is especially true for the early life stages of cold-water fish, such as Atlantic salmon (Jonsson and Jonsson 2009). In addition to temperature, climate variability influences the recruitment of Atlantic salmon through effects on river flow (Hvidsten et al. 2015; Jonsson and Jonsson 2017), which is projected to go on decreasing in southern Europe, including the Iberian Peninsula (Schewe et al. 2014). Therefore, understanding the underlying causes of the continuous decline of the southernmost European salmon stocks requires an analysis of the long-term changes in the biophysical conditions of their environment in three separate spatial domains: the East and West NA Ocean and the rivers of northern Spain.

The conservation of southern European freshwater basins is of concern, owing to the high physiological sensitivity to warming and low evolutionary potential of their fishes, concurrent with high levels of human impact (Comte and Olden 2017*b*). Atlantic salmon is not an exception. The conservation of the southernmost European populations requires rigorous management rooted in a clear understanding of the factors driving the ongoing decline. The purpose of the present study was therefore to investigate the temporal abundance trends of Atlantic salmon stocks in Spain over 62 years and to identify potential links to current climatic changes in their feeding and breeding areas. We tackled these general objectives by addressing the following specific research questions: (*i*) Has the abundance of returning salmon changed over the study period, and are possible changes consistent across natal rivers? (*ii*) Has the surface temperature in the NA basin changed over the study period, and are possible changes linked to observed trends in global climatic variables? (*iii*) Have the changes in oceanic conditions led to regime shifts in salmon's feeding resources at ocean, such as zooplankton abundance? (*iv*) Have both local temperature and hydrological conditions in the natal fresh waters changed over time? (*v*) Are changes in salmon abundance linked to changes in the climatic and biological conditions in the NA basin and the hydroclimatic local conditions, and what are the main drivers of the Spanish salmon decline?

Materials and methods

Salmon captures

We analyzed 62 years (1950–2011) of returning salmon captured annually from March to July in nine salmon rivers in northern Spain (Eo, Porcía, Esva, Navia, Nalón, Narcea, Sella, Cares, and Deva). The study rivers are small basins with their headwaters very close to the coastline and similar hydrographic characteristics. The latitude of all the basins is ~43°N. The main river course is usually short, almost always less than 150 km in length, with pronounced slopes (mean 1.7%). The Navia and Nalón rivers have mean annual flows exceeding 50 $m^3 \cdot s^{-1}$, while in the rest of the basins the mean annual flow is less than 20 $m^3 \cdot s^{-1}$. Historically, these rivers were grouped into five hydrological units: (1) River Eo (drainage area 828 km^2), (2) Western basins (Rivers Porcía, Esva and Navia; 3182 km^2), (3) Rivers Nalón and Narcea (4827 km^2), (4) River Sella (1284 km^2), and (5) Rivers Cares and Deva (1136 km^2). They are coherent drainage entities that include neighboring river basins that drain to the same estuary (Fig. 1). The local management authorities have regularly and accurately collected Atlantic salmon catch per unit effort (CPUE) data through the study area every year since 1949. This is the only measure of Atlantic salmon abundance that has been recorded in Spanish rivers over time. There are two minor drainage basins (Eo and Western basins) that represent 8%–10% of historical salmon catches, whereas the rest of study basins contribute with 25% (Nalón–Narcea), 30% (Sella), and 27% (Cares–Deva) to total catches. Moreover, the ratios of captures among basins are similar over time. The relationship between 1SW and MSW salmon catches and its temporal trend is similar across study rivers. The proportion of 1SW salmon rose from 9% to 35% over the study period. This increase in the proportion of 1SW salmon in the population is known as grilsification and has been a generalized process throughout the range of the species. CPUE from recreational salmon fisheries is used as an indicator of abundance when these data are not available (e.g., Vøllestad et al. 2009; Beaugrand and Reid 2012). Fishing regulations for salmon have not changed substantially over the study period. The fishing season lasts from March to July, minimum size limit ranged from 40 to 45 cm, while bag limit is usually one salmon per angler and day. The number of fishing licenses in the study area has not changed significantly over time (period 1971–2015; Mann–Kendall test corrected to account for temporal autocorrelation, $\tau = -0.036$, $p = 0.68$), and it is reasonable to assume that the fishing effort has remained stable. Moreover, cross-correlation analyses showed that the number of fishing licenses and salmon catches were not significantly correlated at any tested lag (10 years) between 1971 and 2011. Therefore, river catches have been used as a proxy for salmon abundance in the present study.

Plankton abundance

The plankton data set (Johns 2017) was obtained from the Continuous Plankton Recorder (CPR) survey operated by the Sir Alister Hardy Foundation for Ocean Science (SAHFOS; see Reid et al. 2003 for details). We analyzed spatial and temporal changes in the abundances of six plankton groups in a spatial domain encompassing 44°N to 65°N and 55°W to 20°E (29 of the CPR standard areas): the phytoplankton colour index was used as an indicator of primary production; zooplankton groups included total small copepods (mostly under 2 mm in length, "traverse" analysis stage),

Fig. 1. Map of the study area.

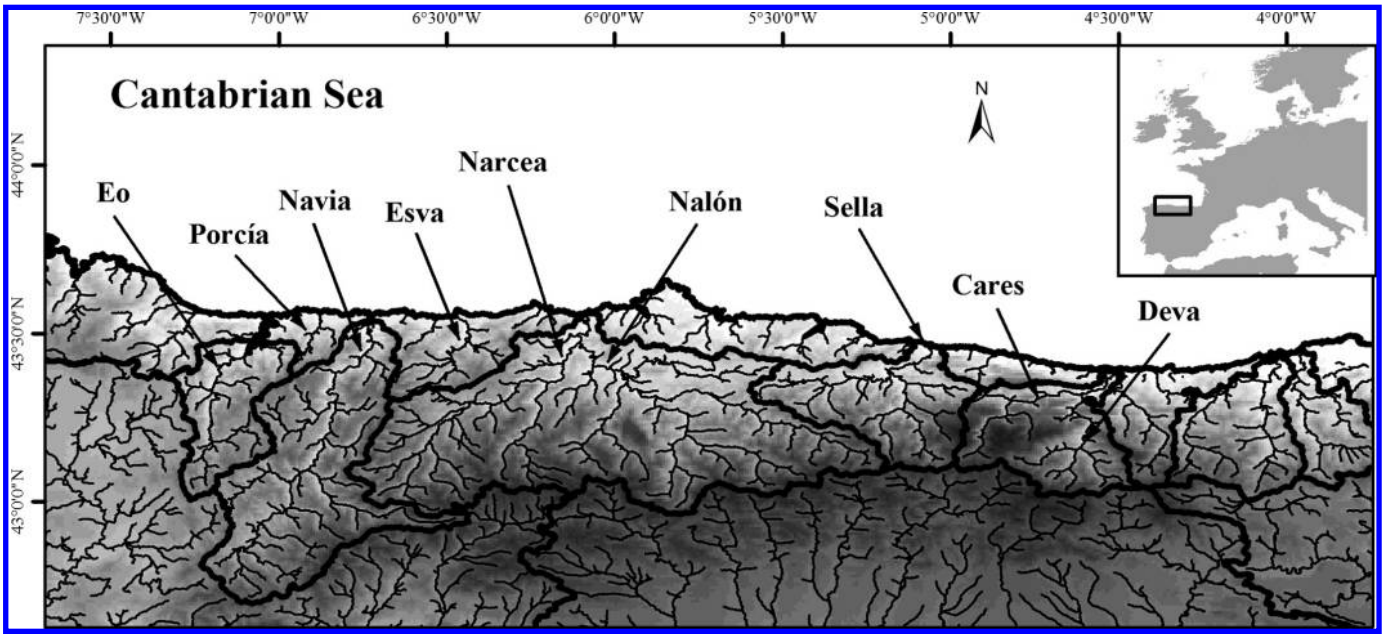

total large copepods (over 2 mm in length, "eyecount" analysis stage), total euphausiids, and two calanoid copepod species that occupy contrasting thermal niches, *Calanus finmarchicus* and *Calanus helgolandicus*. The time series for small copepods and euphausiids covered the period 1950–2011, while data for the rest of the groups were only available from 1958.

Large-scale climate indicators and sea surface temperature (SST)

Land–ocean temperature anomalies (°C) relative to a 1961–1990 reference period for the Northern Hemisphere (NHT) on a 5° latitude × 5° longitude grid resolution from 1860 to 2016 were provided by the UK Meteorological Office Hadley Centre – University of East Anglia Climatic Research Unit (HadCRUT4 data set, http://www.metoffice.gov.uk/hadobs/hadcrut4; Morice et al. 2012).

Two climate indices were used to characterize the natural climatic oscillations in the North Atlantic: the Atlantic Multidecadal Oscillation (AMO) index to characterize the multidecadal mode of climate variability and the North Atlantic Oscillation (NAO) index to describe the intradecadal cycles. Time series of the unsmoothed AMO index for 1860–2016 were obtained from the National Oceanic and Atmospheric Administration (NOAA) website: http://www.esrl.noaa.gov/psd/data/timeseries/AMO/. The AMO index is defined as the SST anomaly based on the Kaplan SST data set (5° × 5° spatial grid resolution) from 0°N to 70°N, linearly detrended to account for the global warming associated with anthropogenic climate change (Enfield et al. 2001). The NAO is a weather phenomenon that measures the difference in the fluctuations in sea-level atmospheric pressure between the subpolar Icelandic low and the subtropical Azores high. Time series from 1865 to 2016 of the Hurrell winter (December through March) NAO index, based on the difference of normalized sea-level pressure between Lisbon (Portugal) and Reykjavik (Iceland), were provided by the National Center for Atmospheric Research (https://climatedataguide.ucar.edu/climate-data/hurrell-north-atlantic-oscillation-nao-index-station-based; Hurrell et al. 2017).

SST data were obtained from the NOAA Extended Reconstruction Sea Surface Temperature (ERSSTv4) data set (https://climatedataguide.ucar.edu/climate-data/sst-data-noaa-extended-reconstruction-ssts-version-4; Huang et al. 2017). The ERSSTv4 data set is based upon statistical interpolation on a 2° × 2° spatial grid of the International Comprehensive Ocean–Atmosphere Data Set (ICOADS) Release 2.5 SST data.

Local-scale climate and hydrological indicators

Local land surface temperature anomalies within the study area from 1950 to 2011 were obtained from the ENSEMBLES daily gridded observational data set for surface temperature in Europe (E-OBS version 13.1; http://www.ecad.eu/download/ensembles/ensembles.php; Haylock et al. 2008). This is a high-resolution (0.25° × 0.25°) daily land data set that uses the European Climate Assessment & Dataset (ECA&D) blended daily station data. We analyzed local temperatures within the study area domain (42.5°N–43.5°N and 4°W–7°W). Annual temperature anomalies were calculated as the difference between the mean daily temperature of the year and the long-term mean temperature (reference value, 1950–2011).

Historical flow variation in the rivers studied was analyzed by means of the indicators of hydrologic alteration, according to Richter et al. (1996) and Olden and Poff (2003). Flow data were obtained from gauging stations placed in the study rivers, where historically, the Spanish Ministry of the Environment has registered daily records. Daily discharge data were processed every year from 1950 to 2011 by IHA 7.1 software (The Nature Conservancy 2009) to obtain 12 indicators that characterize the different dimensions of the flow regime in each river. Flow magnitude was characterized for both the average annual mean daily flow (Mean) and extreme water conditions, measured as the annual minimum and maximum mean discharge during 7 (7Dmin and 7Dmax) and 30 (30Dmin and 30Dmax) consecutive days. Summer low flows are negatively linked to reduced recruitment, growth of Atlantic salmon parr and smolts, affect the timing of river entry, and disrupt upstream migration for reproduction (Jonsson and Jonsson 2011). Minimum low flows were highly correlated to other flow metrics, such as frequency of extreme low-flow events, annual baseflow, or baseflow during the upstream migration period, which were thus not included in the analyses. Maximum flows are typically reached in winter and can impact the smolt migration, both behaviorally and physically by displacing smolts downstream at inadequate timing (Jonsson and Jonsson 2011). The rate of change in discharge was measured as the mean rate of all positive (rise rate, Rr) and negative (fall rate, Fr) changes in discharge between consecutive days. The frequency of water condition changes was measured by the number of hydrologic reversals (Rev), calculated as the number of times that

discharge changed between rising and falling periods. These three metrics characterize flow stability, which is especially important for reproduction, as spawners do not breed when flows are unsteady. Flow fluctuations place redds at risks of dewatering or can cause scouring mortality. In addition, while salmon need high flows to enter the river, they prefer falling phases to ascend a river. Upstream migrations halt at very high flows (Jonsson and Jonsson 2011). The frequency and duration of high (HpF and HpD) and low (LpF and LpD) flow pulses provided a combined variability measure, which can have effects on salmon in rivers. High and low pulses refer to hydrologic events wherein the daily discharge increases above the 75th percentile or drops below the 25th percentile of all daily flows. Calculated time series were normalized by removing the long-term mean and dividing by the long-term standard deviation and then averaged across the eight rivers studied to obtain a single time series for each hydrologic indicator.

Statistical analyses

We performed a wide range of statistical analyses to tackle the research objectives. First, to prepare the data prior to time series analyses, we used principal component analyses (PCAs) to synthesize spatial and temporal variations in SST and abundance of plankton groups across the NA basin. Second, we performed different univariate time series analyses to characterize temporal patterns in study variables, including (*i*) Mann–Kendall tests to identify significant trends in biological and hydroclimatic variables, as well as sequential analyses to detect when regime shifts took place in the series, and (*ii*) singular spectrum analyses to decompose the time series and quantify the different types of variability (trend and cyclic behavior). Third, to characterize relationships between ecosystem components, we used both univariate (correlation analyses) and multivariate analyses, including (*i*) multivariate autoregressive state-space models to simultaneously capture interdependencies between trajectories of salmon populations and their food resources (plankton), as well as their differential responses to hydroclimatic drivers, and (*ii*) chronological clustering to detect common patterns in all time series and identify regime shifts at the ecosystem level. All statistical analyses were performed in R 3.3.3 (R Core Team 2017).

Spatially standardized PCA

We used a spatially standardized PCA to summarize long-term and spatial changes in SST for 1860–2016 over the NA sector comprising 20°N to 74°N and 90°W to 20°E.

Six additional spatially standardized PCAs were performed to identify both long-term temporal and spatial patterns in abundance of plankton groups. We used the log-transformed time series (1950 (or 1958) to 2011) of total abundance in each CPR standard area as input variables. Since the data provided by SAHFOS indicated monthly abundances, we calculated the annual mean for each area, excluding years with monthly data missing for more than 4 months. We then excluded CPR standard areas with less than 20 annual data items and used the regularized iterative PCA algorithm implemented in the missMDA version 1.11 R package (Husson and Josse 2017) to impute the missing entries of the resulting data set.

Finally, we performed a PCA combining the spatiotemporal data from all plankton groups; that is, the input matrix was the result of combining the six matrices used in the previous analysis so that the columns represented abundance time series of all plankton groups in all nonexcluded CPR standard areas.

All PCAs were carried out using the FactoMineR version 1.36 R package (Husson et al. 2017). The first two PCs taken from each of the eight spatially standardized PCAs were used in subsequent analyses.

Trends and regime shifts in time series

We first used the nonparametric Mann–Kendall test (Mann 1945; Kendall 1975), as modified by Yue et al. (2002) to account for serial autocorrelation, to detect significant annual trends of abundance of salmon and plankton groups and of hydroclimatic indicators. This analysis was performed with the zyp version 0.10-1 R package (Bronaugh and Werner 2015).

We then applied two different methods to detect regime shifts in the univariate time series. Beaugrand (2004) pointed out that the commonly observed nonsynchronicity between taxonomic groups in their responses to environmental drivers often originates from the type of statistical techniques applied to detect a shift. Therefore, we considered a main shift to occur when we detected such a shift with both methods and a secondary one to occur when it was only detected with either of the two methods. First, we used a split moving-window boundary analysis (Webster 1973), which computes the statistical contrast of the means of two halves of a window as it moves along the time series. We used a window width of 16 years and detected significant differences between halves through ANOVA tests (α = 0.01). Second, we applied Rodionov's sequential algorithm version 3, in which a first-order autoregressive model (AR1) is used to consider temporal autocorrelation; AR1 was calculated through the method of inverse proportionality with four corrections and a subsample size of 6 years (Rodionov 2006). We used a cut-off length of 12 years (only regimes longer than this threshold are thus detected) and a significance level of α = 0.01. Huber's weight parameter, which controls the weights assigned to the outliers, was fixed at 1.

Decomposition of time series

We employed the singular spectrum analysis (SSA) nonparametric method to decompose the time series of all variables and thus identify the different sources of variability to separate long-term trends from low-frequency cycles and high-frequency fluctuations. We used the Rssa version 0.14 R package (Korobeynikov et al. 2016) to sequentially decompose the time series, group-correlate eigenvectors, estimate the periods of extracted cyclic components, and reconstruct the extracted long-term trend and significant low-frequency components, following the procedures described by Golyandina and Korobeynikov (2014).

Univariate relationships between ecosystem components

We carried out univariate correlation analyses to explore relationships in both original time series and reconstructed series of long-term trend and low-frequency components between (*i*) salmon captures and all biological and hydroclimatic variables, (*ii*) abundances of plankton groups and large-scale hydroclimatic variables, and (*iii*) SST and large-scale climate indicators. We tested the effects of biologically relevant lags (up to 5 years) in flow variables on salmon captures. As in previous analyses, probabilities were estimated accounting for serial autocorrelation. As pointed out by Pyper and Peterman (1998), there is a reduction in the degrees of freedom for a sample correlation between two strongly autocorrelated time series compared with that assumed under the classical significance test ($N - 2$; N being the sample size), so we computed the adjusted effective degrees of freedom and critical value for significance using the Chelton (1984) method, autocorrelations being estimated over the first $N/5$ lags through the Box and Jenkins (1976) function, as described in Pyper and Peterman (1998).

Multivariate relationships between ecosystem components

We first fitted time-invariant multivariate autoregressive state-space (MARSS) models to time series of salmon, plankton, and environmental variables using the MARSS version 3.10.10 R package (Holmes et al. 2018). This analysis was performed to simultaneously estimate the biological interaction strengths in the salmon food web and the effect of abiotic drivers on its dynamics.

Fig. 2. Long-term changes in catch per unit effort (CPUE) (moving average) of Atlantic salmon in the study area (captures from main basins, left *y* axis; total captures, right *y* axis) from 1950 to 2011. The dashed vertical lines indicate the periods (1970–1971; 1989–1990) when a significant shift was detected in the total trend.

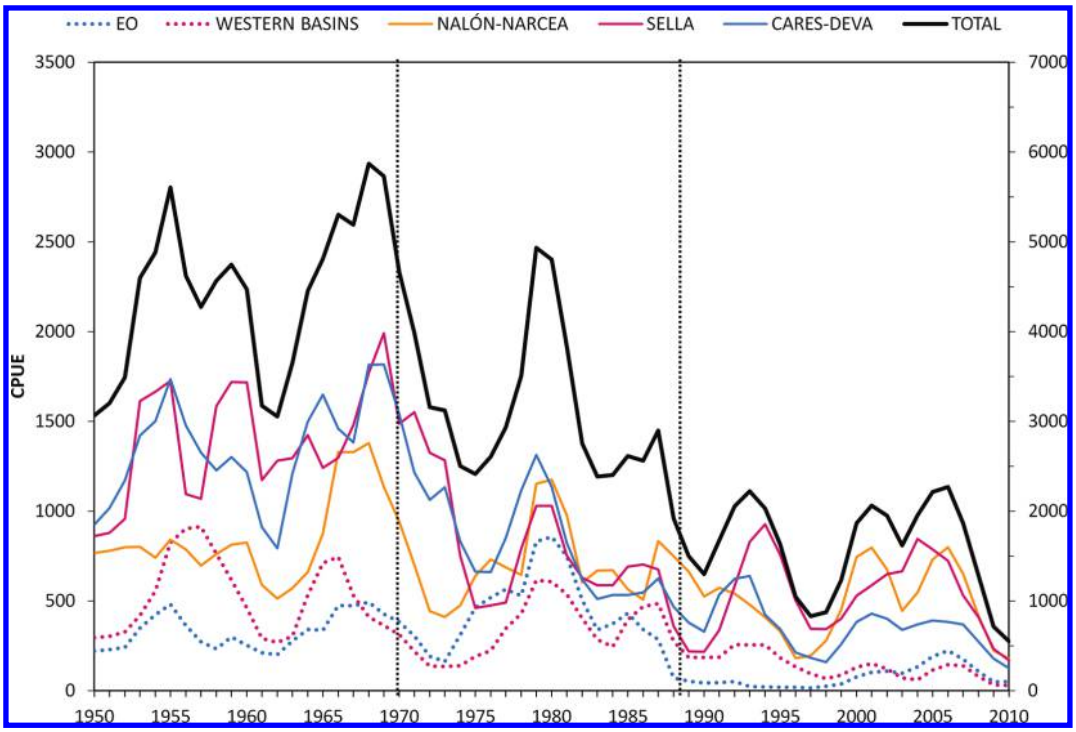

The MARSS model includes a state model and an observation model. The state component, which accounts for process uncertainty caused by unobserved factors, is a multivariate first-order autoregressive (MAR-1) process. It is expressed as

$$(1) \qquad \boldsymbol{X}_t = \mathbf{B}\boldsymbol{X}_{t-1} + \boldsymbol{u} + \mathbf{C}\boldsymbol{c}_t + \boldsymbol{W}_t$$

where $\boldsymbol{X}$ is an $m \times 1$ vector of state values for each of the m biological components of the system (salmon and plankton groups); $\mathbf{B}$ is the $m \times m$ matrix of interactions among biological components, the diagonal coefficients being the first-order autoregressive terms; $\boldsymbol{u}$ is an $m \times 1$ vector describing the mean trend or mean level of state processes; $\boldsymbol{c}_t$ is a $p \times 1$ vector of state covariates (environmental drivers) whose effects map to the states according to the $m \times p$ matrix $\mathbf{C}$; and $\boldsymbol{W}_t$ is an $m \times 1$ vector of process errors.

The multivariate observation model, which accounts for the effect of mismeasurement of observed variables, takes the form

$$(2) \qquad \boldsymbol{Y}_t = \mathbf{Z}\boldsymbol{X}_t + \boldsymbol{a} + \boldsymbol{V}_t$$

where $\boldsymbol{Y}_t$ is an $m \times 1$ vector of observed abundances of biological components at time t; $\mathbf{Z}$ is an $m \times m$ matrix connecting observed time series with corresponding processes; $\boldsymbol{a}$ is an $m \times 1$ scaling vector; and $\boldsymbol{V}_t$ is an $m \times 1$ vector of measurement errors. Both $\boldsymbol{W}_t$ and $\boldsymbol{V}_t$ are assumed to follow multivariate normal distributions with zero means and variances $\mathbf{Q}$ and $\mathbf{R}$, respectively.

We used time series of salmon captures and the first two components from the PCA synthesizing the spatiotemporal data from all plankton groups (see previous section on Spatially standardized PCA) as observed values ($\mathbf{Y}$ matrix). We used time series of the environmental drivers that were significantly correlated with salmon captures as state covariates ($\boldsymbol{c}$ vector). For flow variables, we used the tested lag with the highest correlation. We standardized all input time series (abundances and covariates) and assumed that the mean of our data ($\mathbf{Y}$) is a good estimate of the mean of the system ($\boldsymbol{X}$), so we could set $\boldsymbol{u}$ and $\boldsymbol{a}$ to zero. $\mathbf{Z}$ was set to the identity matrix. We set all off-diagonal coefficients in matrices $\mathbf{Q}$ and $\mathbf{R}$ to zero and assumed that coefficients for plankton groups were the same. The $\mathbf{B}$ and $\mathbf{C}$ matrices were thus the main elements of the model to be estimated. Local environmental drivers only affected salmon so the other terms corresponding to plankton groups in the $\mathbf{C}$ matrix were set to zero. We did not model interactions between zooplankton groups, so corresponding elements in the $\mathbf{B}$ matrix were set to zero. We fitted the model to all potential combinations of model inputs (state variables and environmental drivers) and selected the best fit based on sample-size-corrected Akaike information criterion (AIC_c) values.

We additionally performed chronological clustering to detect homogeneous temporal periods in the complete multivariate data set for the abundance of salmon and six plankton groups (the first two PCs originated from the spatially standardized PCAs) and large-scale and local hydroclimatic indicators (including the first two PCs derived from the PCA on SST). Chronological clustering differs from regular agglomerative hierarchical clustering in that it is time-constrained to preserve the sequence of years when homogeneous groups are detected (Legendre et al. 1985). We clustered the input Euclidean distance matrix using the CONISS agglomeration method (Grimm 1987) implemented in the rioja package for R version 0.9-15 (Juggins 2017). The number of significant clusters was defined by comparing the dispersion of the hierarchical classification obtained with that calculated from a broken-stick model (Bennett 1996). In this approach, clusters are retained if their dispersion values are higher than the corresponding random broken-stick components.

Results

Long-term changes in Atlantic salmon abundance

Total Atlantic salmon abundance in northern Spanish rivers showed a significant negative trend over the 1950–2011 period (Mann–Kendall test $\tau = -0.493$, adjusted Kendall p value < 0.0001).

Fig. 3. Net change in sea surface temperature (°C) for four 15-year periods in the North Atlantic, based on the annual rate of change as measured by Sen's slope (left column). Anomaly in sea surface temperature (°C) was estimated as the averaged sea surface temperature in each period minus the averaged sea surface temperature from 1860 through 1949 (right column). Land areas of Europe and North America are shown in grey.

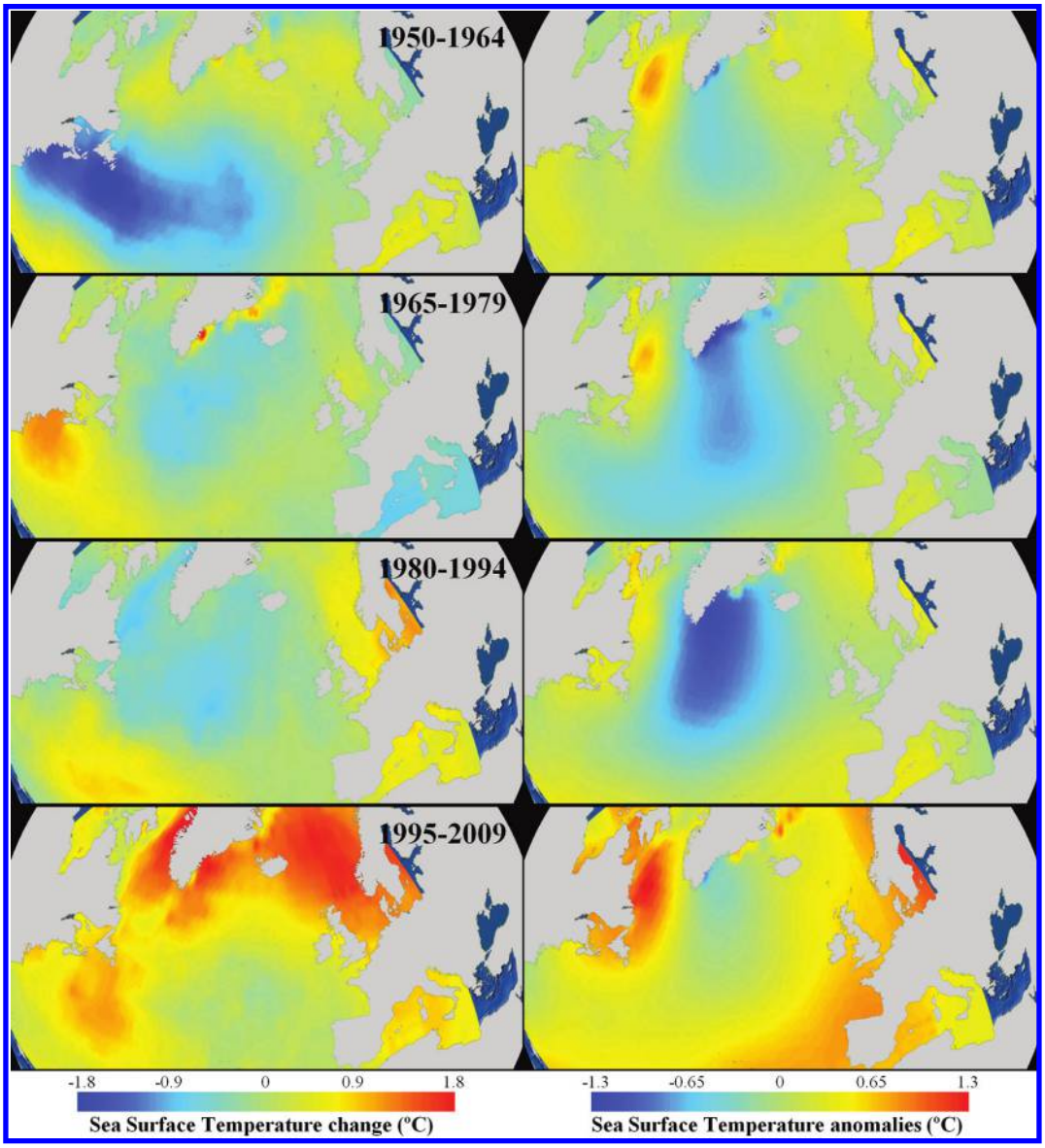

The same trend was observed when the river basins were analyzed separately (Eo: $\tau = -0.330$, $p < 0.0001$; Western basins: $\tau = -0.518$, $p < 0.0001$; Nalón–Narcea: $\tau = -0.248$, $p < 0.001$; Sella: $\tau = -0.410$, $p < 0.0001$; Cares–Deva: $\tau = -0.588$, $p < 0.0001$) (Fig. 2). The long-term tendency extracted through SSA explained 85.4% of the variability of salmon stocks over time (see online Supplementary materials, Table S1[1]). There was a weaker shift in 1970–1971 followed by a strong decline from 1989 (Fig. 2). Abundance during the 1950–1970 period (mean = 4500.8 ± 1341.7, coefficient of variation (CV) = 29.8%) was 30.6% higher than during the 1971–1988 period (mean = 3123.9 ± 1441.1, CV = 46.2%). Finally, salmon stocks were further reduced by 51.3% from 1989 onwards (mean = 1520.9 ± 1441.1, CV = 46.0%).

Long-term changes in NA climate and SST

Mean SSTs in the NA showed significant interdecadal variability and marked changes in trend during the study period (Fig. 3). There were, however, marked spatial differences in trends, 1995–2009 being the only period when warming was consistent throughout the NA. Overall, there was a net cooling in the central oceanic waters, but increased net temperatures elsewhere, warming being stronger in the Baltic and Norwegian seas, along the coasts of Spain and France and, especially, at West Greenland and in the Labrador Sea, where temperature anomalies were over 1 °C (Fig. 3).

The time series of the first PC from the spatially standardized PCA performed on SST (SST PC1; 39.14% of the total variance) was dominated by the NHT warming signal (r = 0.86, adjusted-

[1]Supplementary data are available with the article through the journal Web site at http://nrcresearchpress.com/doi/suppl/10.1139/cjfas-2018-0297.

Fig. 4. Correlation analyses between sea surface temperatures (SSTs) and Northern Hemisphere temperature (NHT) anomalies (left column) and the Atlantic Multidecadal Oscillation (AMO) index (right column) for the period 1860–2016 (first row). Spatial representation of correlation analyses between SST and the first (left column) and second (right column) principal components from a standardized PCA for 1860–2016 are shown in the second row. The bottom panels show long-term changes in the first principal component of SST (blue line) and NHT anomalies (red line) (r = 0.86; bottom left) and the second principal component of SST (blue line) and the AMO index (red line) (r = 0.50; bottom right) for 1860–2016.

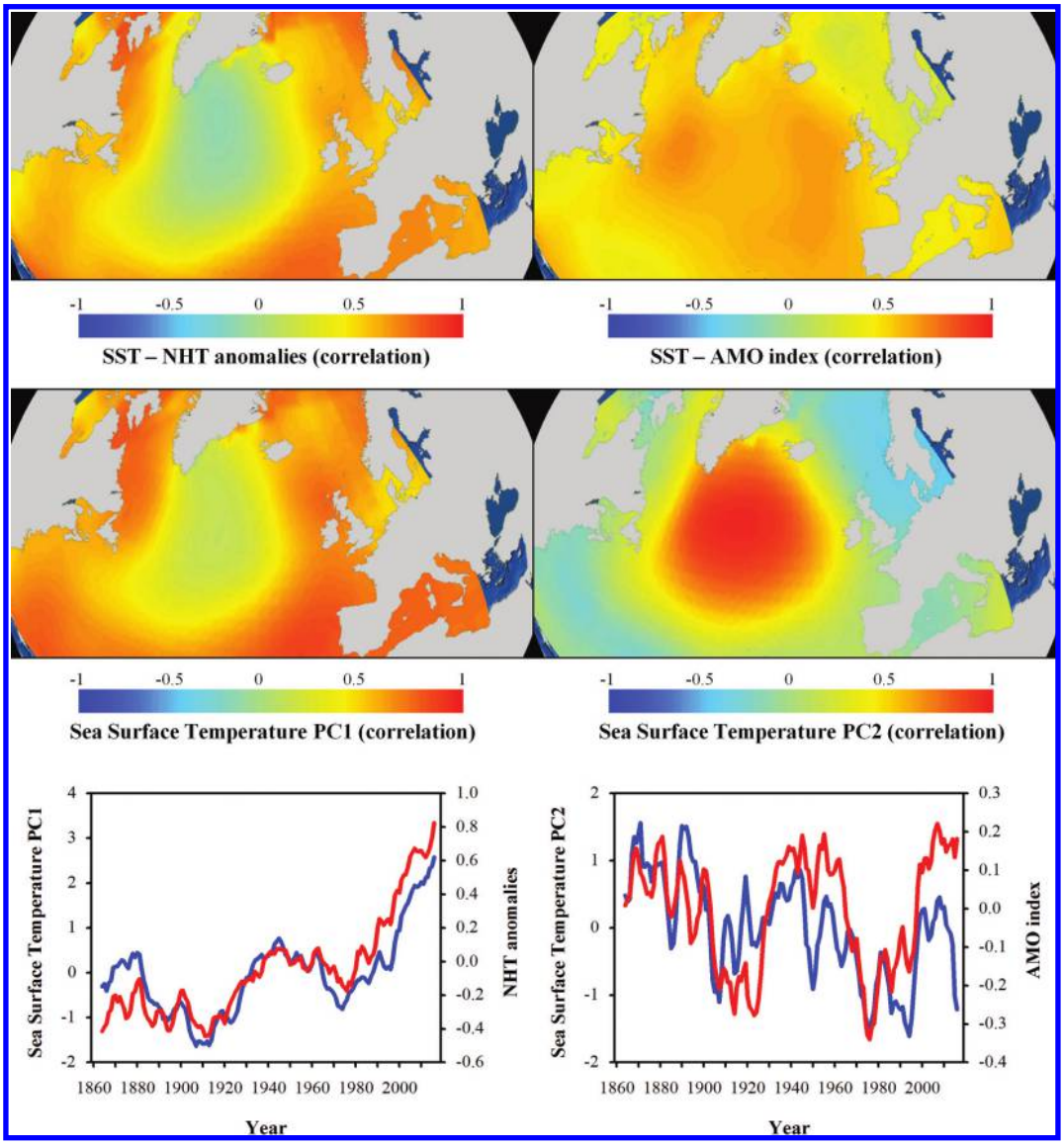

p < 0.0001) from 1860 to 2016 (Fig. 4). SSTs were highly, positively correlated with the first PC in all areas of the NA but the central oceanic waters, in which the oscillatory signals were prevalent (Fig. 4). The second PC (SST PC2; 12.27%) was dominated by the AMO signal (r = 0.50, adjusted-p < 0.0001) and reflects the opposition between the central areas that have experienced net cooling or weak warming and the warmed surrounding areas (Figs. 3, 4).

In consequence, the long-term trend components of SST PC1 and NHT identified through SSA, which represented 70.9% and 71.9% of the variance of the time series, respectively (Supplementary materials, Table S1[1]), were strongly correlated over the period 1950–2011, the correlation coefficient being close to 1 (Table 1). SST PC1 also contained some oscillatory behavior with periods like those of the AMO, and thus long-term trends and low-frequency components were significantly correlated (Table 1). However, the multidecadal variability of the AMO was best captured in the second PC, as the correlation coefficient between long-term trends was over 0.9 (Table 1).

We detected a major shift in the SST PC1 time series towards negative values in 1964, concomitant with both the shift in the AMO to a negative phase and a shift to negative NHT anomalies (Fig. 5; Supplementary materials, Fig. S1[1]). SST PC1 continued with negative values until 1986, when a regime shift linked to an abrupt shift to positive values in the NHT anomalies occurred. The increasing trend in SST PC1 was reinforced, and the rate of change sped up from 1996 onwards, due to the synchronized, pronounced increase in NHT anomalies and the shift of the AMO to positive phase (Figs. 3, 5). The shifts exhibited by SST PC2 paralleled the 1964 (with a 3-year lag) and 1996 phase shifts observed in the AMO (Fig. 5).

Table 1. Correlations between sea surface temperature (SST) and large-scale climatic variables reconstructed by singular spectrum analysis using the eigenvectors representing the long-term trend (T) and various low-frequency cyclic components (C, C1, C2, C3) with different periods (indicated in parentheses) for the period 1950–2011.

	NHT			AMO			Winter NAO	
	T	C1 (9.4)	C2 (66.6)	T (65.8)	C1 (9.2)	C2 (19.1)	T (66.4)	C (7.6)
SST PC1 T	**0.97**	0.00	−0.02	**0.68**	−0.02	0.03	0.33	0.00
SST PC1 C1 (17.9)	−0.10	0.07	0.06	0.34	0.06	**0.61**	−0.18	0.04
SST PC1 C2 (7.3)	0.03	0.35	−0.05	−0.03	0.21	0.07	−0.03	**0.55**
SST PC1 C3 (10.0)	−0.04	**0.47**	0.15	−0.04	**0.72**	0.16	0.06	0.19
SST PC2 T (70.4)	0.49	0.05	−0.22	**0.92**	0.02	0.00	−0.27	0.02
SST PC2 C1 (17.0)	−0.03	0.12	0.07	0.01	0.16	0.49	−0.03	0.00
SST PC2 C2 (8.5)	−0.04	0.27	0.18	−0.02	**0.71**	0.16	0.05	−0.01
SST PC2 C3 (11.0)	0.05	−0.42	0.03	−0.09	−0.33	0.21	−0.04	−0.12

Note: Significant correlations ($p < 0.05$) after accounting for temporal autocorrelation are marked in bold. NHT, Northern Hemisphere temperature; AMO, Atlantic Multidecadal Oscillation; NAO, North Atlantic Oscillation.

Fig. 5. Long-term changes in large-scale and local hydroclimatic variables over the 1950–2011 period. Solid and dashed vertical lines indicate main and secondary regime shifts, respectively, estimated by split-moving window boundary analysis and Rodionov's sequential algorithm.

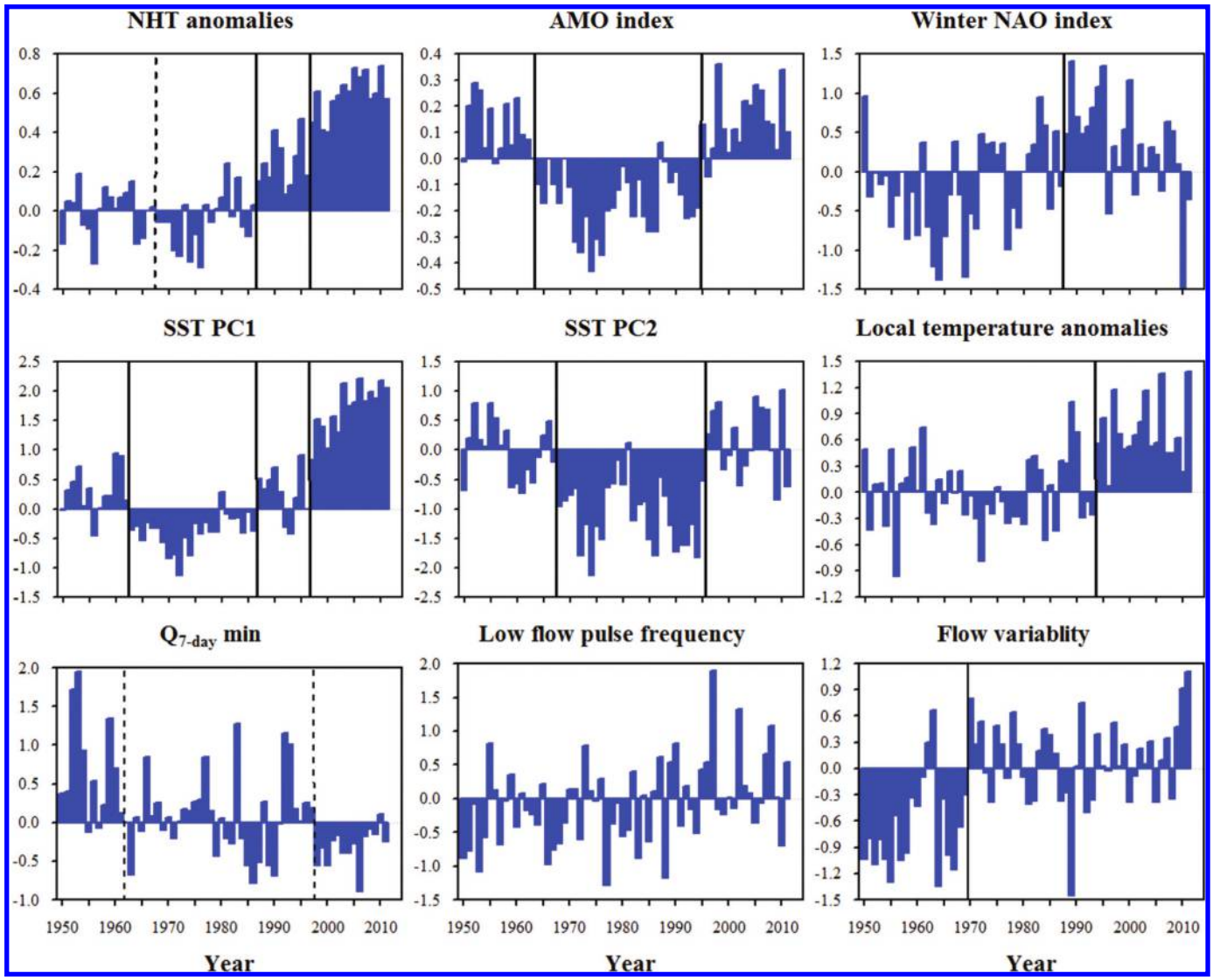

Long-term changes in plankton abundance and potential drivers of change

Typically, the first eigenvectors of the PCAs performed on plankton groups were significantly and positively correlated with the abundances of taxa studied in the different CPR standard areas (i.e., significant correlations were characteristically positive; Supplementary materials, Fig. S3[1]). They thus reflect the long-term changes in net abundances in the NA, although there were marked spatial differences in trends. There were also differences in the contribution to the PC1s between areas located in the West and East NA. Variance explained by PC1 ranged from 13.1% (large copepods) to 52.6% (phytoplankton). All second eigenvectors were

Fig. 6. Long-term changes in salmon and plankton (first principal components) abundance over the 1950–2011 period (blue bars, left axes). Long-term change in the first principal component of sea surface temperature is also shown in each graph (red line, right axes). Solid and dashed vertical lines indicate main and secondary regime shifts, respectively, estimated by split-moving window boundary analysis and Rodionov's sequential algorithm.

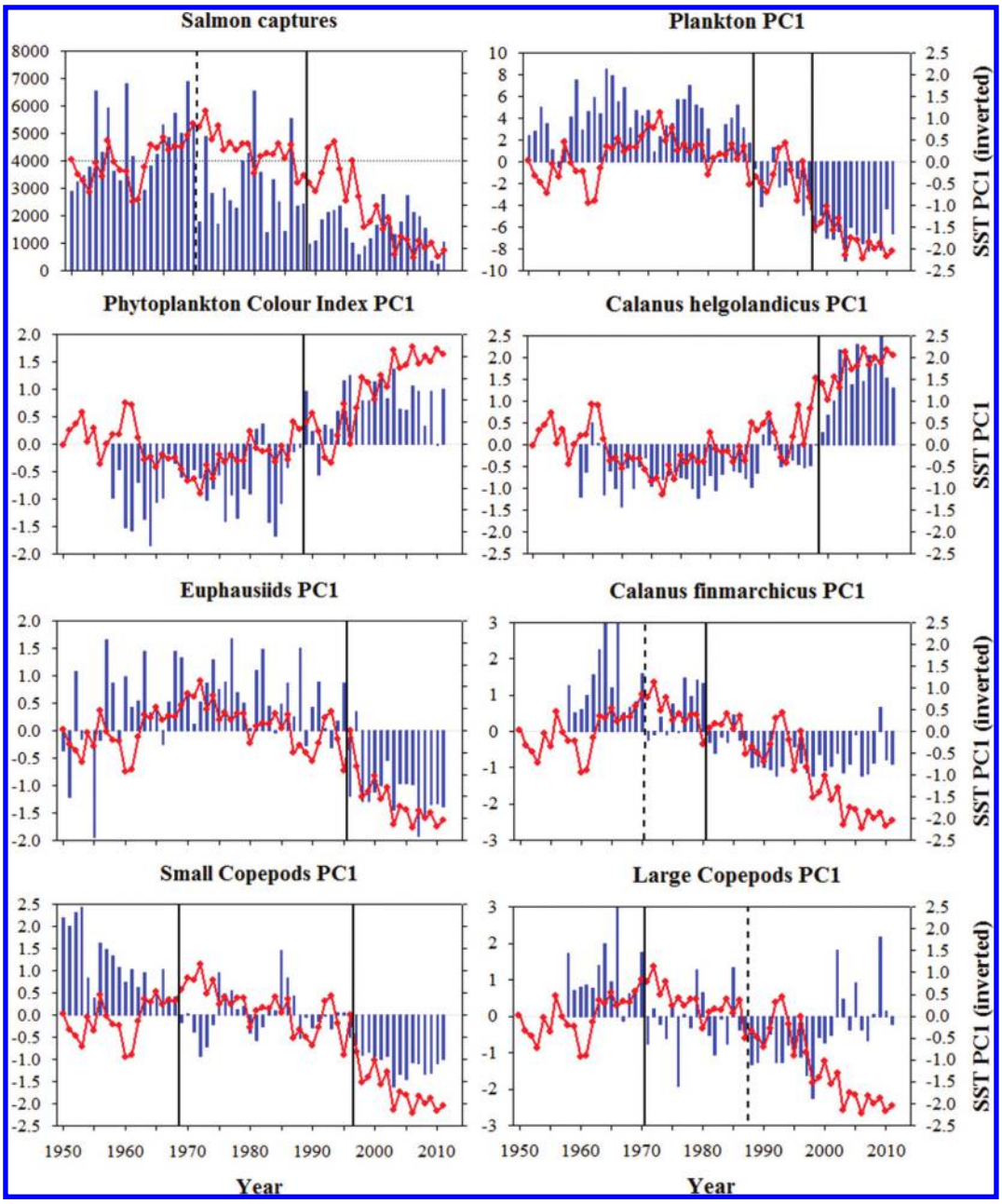

positively correlated with plankton abundances in certain CPR standard areas, but negatively in others. This reflected the opposite oscillatory trends in the West and East NA (Supplementary materials, Figs. S3, S4[1]). Variance explained by PC2 ranged from 9.2% (small copepods) to 23.7% (euphausiids).

Abundances of plankton groups (PC1) exhibited significant negative trends, except for phytoplankton and *C. helgolandicus*, whose abundance significantly increased over time (Mann–Kendall test; adjusted Kendall p value < 0.0001, except for large copepods: $p < 0.01$). The long-term trend extracted through SSA explained between 36.8% (*C. finmarchicus*) and 78.4% (*C. helgolandicus*) of temporal variations in the abundances of plankton groups (Supplementary materials, Table S1[1]). We detected regime shifts in time series of all plankton groups, but the timing differed across taxa (Fig. 6; Supplementary materials, Fig. S2[1]). Shifts took place mostly in the 1980s and 1990s, although first changes in abundance trends of small and large copepods started earlier. Shift patterns were consistent across the West and East NA, except for euphausiids, whose decline started earlier in time (mid-1980s) in the East NA (Supplementary materials, Fig. S5[1]). When plankton groups were analyzed together, the main regime shifts were found in the late 1980s and mid- to late 1990s (Fig. 6).

The long-term trends, extracted through SSAs, in plankton abundances (PC1s) were significant and highly negatively correlated with trends in NHT anomalies and SST (PC1), except for phytoplankton and *C. helgolandicus*, which correlated positively (Supplementary materials, Table S2[1]). The correlations of time series of biological groups and SST showed marked spatial varia-

Table 2. Correlations between the 1950–2011 time series of salmon captures and global and local hydroclimatic and biological variables, as well as the series reconstructed by singular spectrum analysis using the eigenvectors representing the long-term trend and the main low-frequency cyclical components (periods indicated in the first column; period of salmon oscillations is 12.8 years).

Variables	Period	Time series	Long-term trend	Cyclical variability
Global climate				
NHT	9.4	**–0.56**	**–0.84**	–0.25
AMO	9.2	–0.13	0.18	–0.19
Winter NAO	7.6	–0.32	**–0.68**	–0.06
SST PC1 (39.1)	7.3	**–0.53**	**–0.72**	0.10
SST PC2 (12.3)	11.0	0.04	0.04	**0.84**
Local climate				
E-OBS	7.2	**–0.53**	**–0.79**	0.00
7Dmin	7.6	**0.30**	**0.61**	–0.02
LpF	5.3	**–0.33**	–0.55*	0.00
Rev	7.4	**–0.34**	**–0.76**	–0.11
Biological				
Phytoplankton PC1 (52.6)	7.0	**–0.53**	**–0.90**	0.10
Euphausiids PC1 (26.7)	8.0	0.32	0.57*	0.10
Small copepods PC1 (37.1)	8.8	**0.45**	**0.91**	0.04
Large copepods PC1 (13.1)	9.8	0.32	**0.81**	–0.05
Calanus finmarchicus PC1 (17.5)	7.7	**0.61**	**0.96**	0.10
Calanus helgolandicus PC1 (22.9)	11.3	**–0.48**	**–0.75**	–0.09
Phytoplankton PC2 (11.8)	9.6	0.14	–0.14	0.00
Euphausiids PC2 (26.1)	6.9	**0.38**	**0.79**	0.29
Small copepods PC2 (9.2)	9.3	**–0.27**	–0.06	–0.07
Large copepods PC2 (11.6)	7.3	**0.43**	**0.72**	0.10
Calanus finmarchicus PC2 (10.8)	10.3	–0.21	0.03	–0.30
Calanus helgolandicus PC2 (13.2)	8.6	–0.06	–0.40	0.15
All plankton variables PC1 (19.3)	9.0	**0.58**	**0.85**	**–0.53**
All plankton variables PC2 (7.1)	18.0	0.26	–0.03	0.10

Note: Significant correlations ($p < 0.05$) after accounting for temporal autocorrelation are marked in bold. The percentage of variance explained by each PC is indicated in parentheses.

*Marginally significant ($p < 0.1$).

tions (Supplementary material, Fig. S6[1]). Although correlations were weaker, the long-term trends of certain plankton groups (phytoplankton, euphausiids, large copepods, and *C. helgolandicus*) were also associated with the trend in the AMO index (Supplementary materials, Table S2[1]).

Cyclical variability in the abundance of plankton groups (represented through the PC2) correlated differently with the natural cycles of hydroclimatic indices (Supplementary materials, Table S2[1]).

Owing to all these patterns, the long-term trend of the first PC summarizing the spatiotemporal patterns of all plankton groups was significantly correlated with the trends in NHT anomalies and SST PC1, while the cyclic variability of the second PC was significantly associated with oscillations of the AMO and SST PC2 (Supplementary materials, Table S2[1]).

Long-term changes in local hydroclimatic variables

Local temperature anomalies showed a significant positive trend during the period 1950–2011 (Mann–Kendall test; adjusted Kendall p value < 0.001) with a major regime shift in 1994 (Fig. 5; Supplementary materials, Fig. S1[1]). Only four of the 12 indicators of hydrologic alteration analyzed showed a significant trend (adjusted Kendall p value < 0.01). The annual frequency of low pulses (LpF), and the annual number of reversals (Rev) showed a significant, positive trend during the 62-year period, whereas the minimum discharge during 7 (7Dmin) and 30 days (30Dmin) followed a significant negative trend. We thus only retained LpF, Rev, and 7Dmin (30Dmin was highly correlated with this indicator) for subsequent analyses. We detected two secondary regime shifts in 7Dmin in the early 1960s and late 1990s and a major shift in Rev in 1970, while no shifts were detected in LpF (Fig. 5; Supplementary materials, Fig. S1[1]).

Relationship between salmon abundances and long-term changes in global and local ecosystem conditions

Regarding environmental drivers, the long-term trend, extracted through SSA, in salmon captures was significantly and negatively correlated with trends in NHT anomalies, SST (PC1), local temperature anomalies (E_OBS indicator), flow variability (Rev), and low-flow pulses (LpF) and positively with trends in minimum flows (7Dmin) (Table 2). Lagged series of LpF and 7Dmin were significantly correlated with time series of salmon captures at least up to the third lag, where maximum correlations were observed (Supplementary materials, Table S3[1]). Cyclic oscillations correlated strongly and significantly with the cyclical variability in SST, whose signal was captured by the second PC. Regarding trophic interactions, the long-term trends in the abundance of most plankton groups (PC1s) and salmon captures were significantly and highly correlated (absolute value of Pearson's $r > 0.75$; Table 2). Both the trends and cyclic components of salmon captures and the first PC summarizing the spatiotemporal patterns of all plankton groups were significantly correlated.

In the multivariate analysis, the MARSS model with the lowest AIC_c value and best fit to data (Fig. 7) did not include E_OBS or Rev variables. Local temperature anomalies indicator did not enter the model because it was highly correlated with SST PC1 (both driven by the global temperature anomalies: NHT), thus both variables were redundant. In the best model, the autoregressive parameters in the matrix of interactions (**B** matrix) indicated strong density dependence in salmon abundance, the process rapidly reverting to the mean, while the opposite was observed for plankton groups (Table 3). Off-diagonal values in the **B** matrix revealed relatively strong positive effects of plankton abundance on salmon, while salmon exerted negative, but weaker, effects on

Table 3. Parameter estimates of the analysis of salmon and plankton abundance trajectories based on the smallest AIC_c multivariate autoregressive state-space model (MARSS).

	B			**C**				**Q**	**R**
	Salmon	Plankton PC1	Plankton PC2	SST PC1	SST PC2	7Dmin	LpF	Process error	Obs. error
Salmon	0.26	0.45	0.51	−0.54	0.06	0.18	−0.16	0.12	0.19
Plankton PC1	−0.19	0.99	0	−0.21	0.08	0	0	0.04	0.24
Plankton PC2	−0.28	0	0.90	−0.20	0.26	0	0	0.04	0.24

Note: **B** is the matrix of autoregressive terms and interaction parameters, **C** is the matrix of effects of hydroclimatic covariates, and **Q** and **R** are the matrices of process- and observation-error variance, respectively. Plankton variables are the first two principal components from the PCA synthesizing spatiotemporal data from all plankton groups (phytoplankton, small and large copepods, euphausiids, and the two species *C. finmarchicus* and *C. helgolandicus*). Lagged (3 years) time series were used for flow variables (7Dmin and LpF) in the analysis.

Fig. 7. Model fit (black solid line) and 95% confidence interval (grey area) of the multivariate autoregressive state-space model for time series of salmon captures. Dots are observed data.

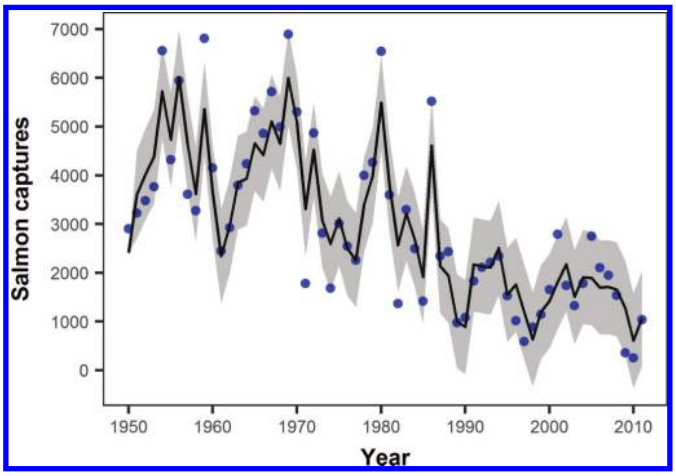

plankton. Values in the matrix of hydroclimatic covariates (**C** matrix) showed that salmon abundance was strongly and negatively influenced by SST PC1 (component of SST dominated by the anthropogenic warming signal), while the effects of flow variables were moderate (Table 3).

When the long-term trends, cyclical variability, and regime shifts of the biological and hydroclimatic components of the NA basin are considered together with local changes in natal fresh waters, a chronological cluster analysis reveals four distinct periods between 1950 and 2011, with major temporal discontinuities after 1964, 1970, and 1986 (Fig. 8). The 1964 break parallels the shifts in the AMO and NHT anomalies, and thus SST, towards cooler phases, which preceded the regime shifts in salmon captures and the abundances of *C. finmarchicus* and small and large copepods circa 1970. From this point, river flows became more unpredictable. The main break occurred in 1986–1987, which led to a period of ever-increasing sea surface and freshwater temperatures, driven by the concurrence of rising NHT anomalies and the positive phase of the AMO, and of sequential changes in all trophic levels of the marine ecosystem, from phytoplankton to salmon through all zooplankton groups studied.

Discussion

Here, we provide evidence indicating that the long-term declining trend in salmon abundance in the southernmost European populations is driven by climate change. The abundance of Spanish salmon experienced an abrupt decrease at the beginning of the 1970s, coinciding with the collapse of the commercial salmon fisheries at West Greenland, the supposed feeding areas of Spanish MSW salmon (Reddin et al. 2012), and the collapse of spring-spawning herring (*Clupea harengus*) in the Norwegian Sea (Gullestad et al. 2014), its meridional region being potentially exploited by southern European 1SW salmon (Jacobsen et al. 2012; Reddin et al. 2012). Despite the subsequent drastic reductions in fishing pressure in the ocean, the abundance of Spanish salmon kept declining and experienced a second abrupt regime shift in 1988–1989. The long-term increasing trend in SST, driven by anthropogenic climate warming in the North Atlantic, was strongly and inversely correlated with the trend for Spanish salmon. The warming trend in SST was also significantly associated with long-term changes in the abundance of all lower trophic levels of the ecosystem studied, shifts that in turn were significantly linked to the decline of salmon. The estimated optimal temperature for postsmolt Atlantic salmon is much higher than the SST in the assumed marine feeding area of Spanish Atlantic salmon. Thus, the current increase in SST should improve the opportunity for growth and the associated survival (Friedland et al. 2000; Jonsson and Jonsson 2004). On the other hand, increased temperatures can lead to decreased growth and suboptimal feeding with reduced survival as a result (Otero et al. 2011; Jonsson et al. 2013). During the first year at sea, Atlantic salmon feed largely on zooplankton (Lear 1980; Jacobsen and Hansen 2001; Haugland et al. 2006). Thus, the decrease in zooplankton biomass concurrent with the increase in temperature may be important for the reduced survival rate of Atlantic salmon at sea (Pauly 1980; Jonsson et al. 2016). However, the increase in SST is too small, between 0.8 and 1.3 °C in relevant areas in 60 years, to produce direct physiological effects, so the ecological regime shift with poorer feeding (e.g., influencing winter survival as hypothesized by Beamish et al. 2004) may be the main reason for the decrease in Spanish Atlantic salmon.

While we detected significant common trends in hydroclimatic drivers and the abundances of plankton groups on the overall NA basin scale, the biological response patterns to hydroclimatic changes were spatially heterogeneous. Total copepods and euphausiids declined while primary productivity (i.e., the phytoplankton colour index) increased over time throughout the Northeast Atlantic. Regarding single indicator species, the abundance of the cold-water copepod *C. finmarchicus* was greatly reduced, especially in the North Sea and south of the Norwegian Sea, while the warm-water species *C. helgolandicus* flourished in the same geographical areas, although never reaching the former numbers of *C. finmarchicus*. These response patterns are consistent with the ecosystem regime shifts described in previous studies of the Northeast Atlantic (e.g., Beaugrand 2009; Friedland et al. 2009; Beaugrand and Reid 2012; Harris et al. 2014). Total copepods comprise both warm- and cold-water species, and, as pointed out by Harris et al. (2014), the negative trend indicates that the replacement of cold-water species by warmer-water ones is not taking place rapidly enough.

Overall, these patterns point towards reduced secondary productivity, with decreased abundance not only of food items directly consumed by salmon (e.g., euphausiids or *C. finmarchicus*; Haugland et al. 2006) but also of those consumed by other species upon which salmon may prey, together with increased primary productivity, reflecting a loss of energy from the ecosystem (Friedland et al. 2009). In addition, the decline in the abundance of zooplankton has been synchronized with the increased abundance of competing pelagic fishes in some systems of the North-

Fig. 8. Chronological cluster analysis of salmon abundance and all-time series of biological and global and local hydroclimatic variables given in Figs. 3, 4, and S5[1]. Bold vertical lines indicate major temporal discontinuities, with the number of significant homogeneous periods estimated by a broken-stick model: (A) 1964–1965: shifts in AMO and NHT trends leading to SST switch to cooler phase; (B) 1970–1971: sharp decrease in salmon abundances and changes in its marine food web, signaled by decreased mean and increased variability in abundance of *C. finmarchicus* and small and large copepods, concurrent with increased unpredictability in river flows; (C) 1986–1987: continually increasing SST and freshwater temperatures driven by rising NHT anomalies and the positive phase of the AMO, linked to changes in abundance of salmon and all lower trophic levels.

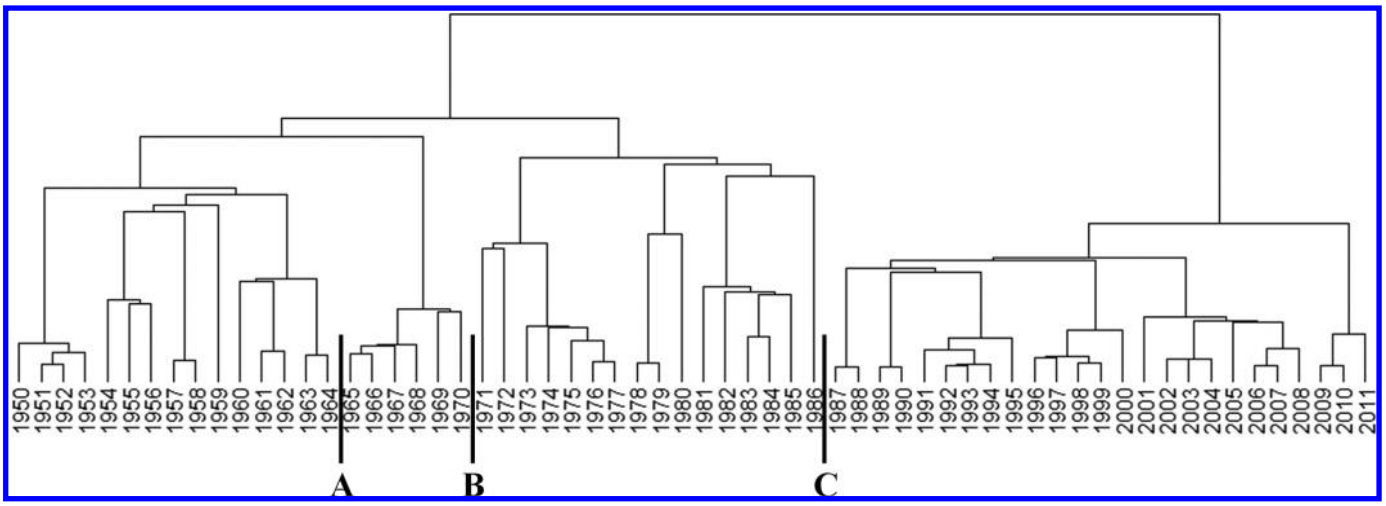

east Atlantic, as in the Norwegian Sea (Jonsson et al. 2016). These ecosystem shifts have been linked to reduced salmon growth at sea, and thus marine survival, in both northern and southern European populations (Friedland et al. 2009; Beaugrand and Reid 2012; Jonsson et al. 2016).

Regarding the Northwest Atlantic, we observed increasing phytoplankton abundance and declining numbers of large copepods, *C. finmarchicus*, and especially euphausiids linked to SST warming in the waters south of Greenland. These patterns agree with the climate-driven ecosystem responses reported by Mills et al. (2013) in the same geographical area. Those researchers showed that while phytoplankton became more abundant, large-bodied lipid-rich species, such as euphausiids and *Calanus* spp., became scarcer; simultaneously, the body size and abundance of capelin (*Mallotus villosus*), a key prey of Atlantic salmon (Jacobsen and Hansen 2001), declined and its distribution changed (Mills et al. 2013). Altered energy flow through the Northwest Atlantic food web has reduced capelin energy density by one-third since the early 1990s (Renkawitz et al. 2015). Atlantic salmon have switched prey, now consuming fewer capelin and more small-sized, lower-energy prey, such as juvenile boreoatlantic armhook squid (*Gonatus fabricii*) and hyperiid amphipods (Renkawitz et al. 2015; Dixon et al. 2017). These responses parallel the reduced abundance and productivity of MSW Atlantic salmon across the Northwest Atlantic (Mills et al. 2013). They might also be linked, together with poorer growth conditions in the Northeast Atlantic during the first year at sea, to the reduced abundance of MSW salmon from southern Europe at West Greenland (ICES 2018).

We showed that long-term trends in the abundance of salmon and plankton groups (PC1s) were highly correlated with that of SST, which was dominated by the NHT warming trend. However, oscillatory behavior, both the long-term trend and the periodic higher-frequency cycles of the AMO, was signaled in the long-term trend of SST as expected, since such oscillation is present in the NHT signal (Schlesinger and Ramankutty 1994). Consequently, the long-term trend of the AMO was significantly correlated with the trend in the abundance of most plankton groups, which adds to the growing body of literature providing evidence of the driving role of the AMO in shaping salmon's marine ecosystems (e.g., Friedland et al. 2009, 2014; Edwards et al. 2013; Mills et al. 2013; Harris et al. 2014). The population abundances of lower trophic levels (phytoplankton and zooplankton) are affected by the AMO through changes in SST (effects on life history, physiology, behavior, and phenology), wind, and current regimes (effects on nutrient availability and passive dispersal). Induced changes can cascade through the food web up to the fish level (review by Nye et al. 2014). Although AMO patterns seem to shape the physical and biological conditions of the salmon's marine environment, time series of AMO and Spanish salmon abundance were directly correlated only during the "warm" (positive) phase of the AMO, which started in the 1970s, as has been observed in recent studies on other populations (Condron et al. 2005; Mills et al. 2013; Friedland et al. 2014). The warm phase of the AMO has reinforced the anthropogenic warming trend to exert both direct physiological and bottom-up trophic effects on salmon populations at sea.

SST changes in the NA are driven by a combination of contemporary climate warming and spatially heterogeneous natural climatic oscillations that have triggered spatially and temporally variable responses from marine organisms over the study period. We detected a regime shift in the physical environment of the NA in 1964–1965 when SST cooled due to a phase shift in the AMO and decreasing NHT anomalies. This shift in physical conditions triggered a biological response that was apparent in a lagged regime shift around 1970. The SST cooling pattern was spatially heterogeneous (SST increased in some NA areas) and led to a period of lower, but more temporally variable, abundances of small and large copepods and a net decrease in *C. finmarchicus* (although there was an increase south of Iceland, as reported by Hátún et al. 2009). This shift is marked by the abrupt drop in Spanish salmon abundance, which is more plausibly linked to widespread overfishing and secondarily to an outbreak of ulcerative dermal necrosis and secondary bacterial and fungal infections in Spain in 1971, which caused high salmon mortality (García de Leaniz and Martínez 1988).

The main regime shift across all trophic levels took place in 1986–1987, with a stepwise increase in SST driven by an abrupt acceleration in anthropogenic warming rates followed by a shift in the winter NAO index. The timing coincided with the previously documented regime shift in the Northeast Atlantic ecosystem (Beaugrand and Reid 2003, 2012). The exceptional warming in the 1980s was global (Myneni et al. 1997) and induced shifts in aquatic — fresh waters (e.g., Hari et al. 2006; Almodóvar et al. 2012) and ocean (e.g., Mills et al. 2013) — and terrestrial ecosys-

tems (e.g., Lenoir et al. 2008). Regime shifts were not synchronized across taxa though, taking place sequentially over the 1980s and 1990s as the SST was continually increasing, due to differences in thermal sensitivities (Beaugrand and Reid 2003, 2012). We detected an abrupt shift in Spanish salmon abundance in 1988–1989, which is consistent with the timing of the collapse in productivity of the southern European stock complex reported by Chaput (2012), just after a general acceleration in declining rates of salmon stocks in the Northeast Atlantic in 1987 (Beaugrand and Reid 2012).

A subtler regime shift occurred in 1995–1996, marked by another stepwise increase in SST, resulting from an abrupt increase in NHT anomalies coupled with a switch to a warm phase in the AMO, entailing a redistribution of warmer and more saline NA water poleward (Hátún et al. 2009). It induced a concomitant negative shift in abundances of small copepods and euphausiids, which agrees with the findings of Beaugrand and Reid (2012), and a lagged boost in abundance of the warm-water species *C. helgolandicus* in the late 1990s.

The shifts described in the marine environment concurred with environmental changes in fresh water. Local temperatures kept rising from the mid-1980s, and at a faster rate from the mid-1990s, following the NHT warming trend. This warming pattern is critical because it is likely to have entailed direct changes in the physiology and behavior of Spanish salmon in their breeding area, in contrast with the trophic-mediated effects of the warming ocean. In addition, flows became more extreme and variable and greatly reduced in summer. These changes in the study catchments started in the 1960s and might be related to the switch to a cool phase in the AMO and the prevalent negative values in the winter NAO index. The warm phases of the AMO correlate with increased summer precipitation in western Europe (Sutton and Hodson 2005), while drier-than-average winter conditions prevailed in southern Europe under high NAO indices (Hurrell et al. 2003). Consequently, conditions after the mid-1960s would involve drier summers, but wetter winters, and thus more variable flows over the year. Anthropogenic climate change might have altered regional patterns, as observed trends in the late 1960s have not been reversed with the change in NAO and AMO phases in the 1980s and 1990s. Instead, precipitation has continued to decline in the study area since the 1970s (González-Taboada and Anadón-Álvarez 2011).

Salmon juveniles in fresh water are sensitive to high water temperatures, which affects their growth and survival (Jonsson and Jonsson 2011). In addition, low summer flows limit salmon recruitment (Jonsson and Jonsson 2017) and smolt production (Hvidsten et al. 2015). Likewise, both outmigration and upstream migration timing are controlled by water temperature and flow conditions (Hansen and Jonsson 1991; Otero et al. 2014). Typically, salmon smolts leave the rivers and begin their migration to the feeding areas at sea during late spring and early summer. The transition from fresh to salt water is critical in the salmon life cycle, as the smolts must adapt to high salinity, cope with new predators, and become accustomed to new types of food. An increase in freshwater temperature implies earlier and shorter migration (Jonsson and Jonsson 2009). In recent years, juveniles in northern Spain have grown slower, smolted younger, and started their seaward migration earlier in the year (A. Almodóvar, unpublished data). By contrast, their return is being delayed, probably because of poorer conditions at sea and the warming of natal fresh waters (Valiente et al. 2011). All these changes would lead to reduced postsmolt survival at sea (Jonsson and Jonsson 2009; Russell et al. 2012; Otero et al. 2014). Our results are thus consistent with simulations predicting that reduced suitable freshwater habitat, due to increased temperatures and reduced flows (Buisson et al. 2008; Lassalle and Rochard 2009), and increased flow variability in synergy with the deterioration of growth conditions at sea (Piou and Prévost 2013) increase the risk of local extinction of southern salmon populations.

Climate-driven environmental changes in the NA and natal fresh waters are driving the decline of the southernmost European salmon populations. Rates of environmental change are high, so the likelihood of their avoiding ultimate extinction depends on their capacity to adapt rapidly, through either phenotypic plasticity or genetic evolution, to the new conditions. Spanish populations have already reacted to ongoing environmental changes through both plastic and genetic responses (Valiente et al. 2010, 2011), and some of them are relatively resilient to such changes (Nicola et al. 2018). However, the fact that effective population size (Horreo et al. 2011*b*) and stock abundance (this study) keep declining suggests that such adaptive responses might not be rapid enough. Many anthropogenic impacts exert selection pressures on the same traits as those influenced by climate change. These may alter evolutionary trajectories or slow down adaptation rates in salmonids (Crozier and Hutchings 2014). Synergies between anthropogenic impact factors accelerate population extinction dynamics in a context of global change (Brook et al. 2008). In our case study, it is evident that the southernmost populations will not withstand current fishing exploitation rates (commercial fishing in the ocean and recreational fishing in fresh waters), while activities reinforcing current climatic trends towards a warmer ocean (increased greenhouse emissions) and warmer and drier fresh waters (e.g., land use change, water abstraction) are likely to accelerate declining rates and might lead to ultimate extinction.

Acknowledgements

The Spanish Ministry of Science and Innovation funded this study through research project CGL2012-36049. We acknowledge the E-OBS data set from the EU-FP6 project ENSEMBLES (http://ensembles-eu.metoffice.com) and thank the data providers in the ECA&D project (http://www.ecad.eu). Special thanks are extended to David Johns from Sir Alister Hardy Foundation for Ocean Science SAHFOS, who provided plankton data recorded by the Continuous Plankton Recorder, SAHFOS. We thank two anonymous reviewers for their constructive comments, which considerably improved the quality of the manuscript.

References

Almodóvar, A., Nicola, G.G., Ayllón, D., and Elvira, B. 2012. Global warming threatens the persistence of Mediterranean brown trout. Glob. Change Biol. **18**(5): 1549–1560. doi:10.1111/j.1365-2486.2011.02608.x.

Beamish, R.J., Mahnken, C., and Neville, C.M. 2004. Evidence that reduced early marine growth is associated with lower marine survival of coho salmon. Trans. Am. Fish. Soc. **133**(1): 26–33. doi:10.1577/T03-028.

Beaugrand, G. 2004. The North Sea regime shift: evidence, causes, mechanisms and consequences. Prog. Oceanogr. **60**(2–4): 245–262. doi:10.1016/j.pocean.2004.02.018.

Beaugrand, G. 2009. Decadal changes in climate and ecosystems in the North Atlantic Ocean and adjacent seas. Deep Sea Res. Part II Top. Stud. Oceanogr. **56**(8–10): 656–673. doi:10.1016/j.dsr2.2008.12.022.

Beaugrand, G., and Reid, P.C. 2003. Long-term changes in phytoplankton, zooplankton and salmon related to climate. Glob. Change Biol. **9**(6): 801–817. doi:10.1046/j.1365-2486.2003.00632.x.

Beaugrand, G., and Reid, P.C. 2012. Relationships between North Atlantic salmon, plankton, and hydroclimatic change in the Northeast Atlantic. ICES J. Mar. Sci. **69**(9): 1549–1562. doi:10.1093/icesjms/fss153.

Beaugrand, G., Edwards, M., Brander, K., Luczak, C., and Ibanez, F. 2008. Causes and projections of abrupt climate-driven ecosystem shifts in the North Atlantic. Ecol. Lett. **11**(11): 1157–1168. doi:10.1111/j.1461-0248.2008.01218.x. PMID: 18647332.

Beaugrand, G., Edwards, M., Raybaud, V., Goberville, E., and Kirby, R.R. 2015. Future vulnerability of marine biodiversity compared with contemporary and past changes. Nat. Clim. Chang. **5**(1): 695–701. doi:10.1038/nclimate2650.

Bennett, K.D. 1996. Determination of the number of zones in a biostratigraphical sequence. New Phytol. **132**(1): 155–170. doi:10.1111/j.1469-8137.1996.tb04521.x.

Box, G.E.P., and Jenkins, G.W. 1976. Time series analysis: forecasting and control. Holden-Day, San Francisco.

Bronaugh, D., and Werner, A. 2015. zyp: Zhang + Yue-Pilon trends package. R Package Version 0.10-1.

Brook, B.W., Sodhi, N.S., and Bradshaw, C.J.A. 2008. Synergies among extinction drivers under global change. Trends Ecol. Evol. **23**(8): 453–460. doi:10.1016/j.tree.2008.03.011. PMID:18582986.

Buisson, L., Thuiller, W., Lek, S., Lim, P., and Grenouillet, G. 2008. Climate change hastens the turnover of stream fish assemblages. Glob. Change Biol. **14**(10): 2232–2248. doi:10.1111/j.1365-2486.2008.01657.x.

Chaput, G. 2012. Overview of the status of Atlantic salmon (*Salmo salar*) in the North Atlantic and trends in marine mortality. ICES J. Mar. Sci. **69**(9): 1538–1548. doi:10.1093/icesjms/fss013.

Chelton, D.B. 1984. Commentary: short-term climatic variability in the Northeast Pacific Ocean. *In* The influence of ocean conditions on the production of salmonids in the North Pacific. *Edited by* W. Pearcy. Oregon State University Press, Corvallis, Oreg. pp. 87–99.

Comte, L., and Olden, J.D. 2017*a*. Evolutionary and environmental determinants of freshwater fish thermal tolerance and plasticity. Glob. Change Biol. **23**(2): 728–736. doi:10.1111/gcb.13427.

Comte, L., and Olden, J.D. 2017*b*. Climatic vulnerability of the world's freshwater and marine fishes. Nat. Clim. Chang. **7**(10): 718–722. doi:10.1038/nclimate3382.

Condron, A., De Conto, R., Bradley, R.S., and Juanes, F. 2005. Multidecadal North Atlantic climate variability and its effect on North American salmon abundance. Geophys. Res. Lett. **32**(23): L23703. doi:10.1029/2005GL024239.

Consuegra, S., García de Leániz, C., Serdio, A.M., González-Morales, M., Straus, L.G., Knox, D., and Verspoor, E. 2002. Mitochondrial DNA variation in Pleistocene and modern Atlantic salmon from the Iberian glacial refugium. Mol. Ecol. **11**(10): 2037–2048. doi:10.1046/j.1365-294X.2002.01592.x. PMID:12296947.

Crozier, L.G., and Hutchings, J.A. 2014. Plastic and evolutionary responses to climate change in fish. Evol. Appl. **7**(1): 68–87. doi:10.1111/eva.12135. PMID:24454549.

Dixon, H.J., Dempson, J.B., Sheehan, J.F., and Renkawitz, M.D. 2017. Assessing the diet of North American Atlantic salmon (*Salmo salar* L.) off the West Greenland coast using gut content and stable isotope analyses. Fish. Oceanogr. **26**(5): 555–568. doi:10.1111/fog.12216.

Edwards, M., Beaugrand, G., Helaouët, P., Alheit, J., and Coombs, S. 2013. Marine ecosystem response to the Atlantic Multidecadal Oscillation. PLoS ONE, **8**: e57212. doi:10.1371/journal.pone.0057212. PMID:23460832.

Enfield, D.B., Mestas-Nunez, A.M., and Trimble, P.J. 2001. The Atlantic Multidecadal Oscillation and its relationship to rainfall and river flows in the continental U.S. Geophys. Res. Lett. **28**(10): 2077–2080. doi:10.1029/2000GL012745.

Finnegan, A.K., Griffiths, A.M., King, R.A., Machado-Schiaffino, G., Porcher, J.-P., Garcia-Vazquez, E., Bright, D., and Stevens, J.R. 2013. Use of multiple markers demonstrates a cryptic western refugium and postglacial colonisation routes of Atlantic salmon (*Salmo salar* L.) in northwest Europe. Heredity, **111**(1): 34–43. doi:10.1038/hdy.2013.17. PMID:23512011.

Friedland, K.D., and Todd, C.D. 2012. Changes in Northwest Atlantic Arctic and Subarctic conditions and the growth response of Atlantic salmon. Polar Biol. **35**(4): 593–609. doi:10.1007/s00300-011-1105-z.

Friedland, K.D., Hansen, P.L., Dunkley, D.A., and MacLean, J.C. 2000. Linkage between ocean climate, post-smolt growth, and survival of Atlantic salmon (*Salmo salar* L.) in the North Sea area. ICES J. Mar. Sci. **57**(2): 419–429. doi:10.1006/jmsc.1999.0639.

Friedland, K.D., MacLean, J.C., Hansen, L.P., Peyronnet, A.J., Karlsson, L., Reddin, D.G., Ó'Maoiléidigh, N., and McCarthy, J.L. 2009. The recruitment of Atlantic salmon in Europe. ICES J. Mar. Sci. **66**(2): 289–304. doi:10.1093/icesjms/fsn210.

Friedland, K.D., Shank, B.V., Todd, C.D., McGinnity, P., and Nye, J.A. 2014. Differential response of continental stock complexes of Atlantic salmon (*Salmo salar*) to the Atlantic Multidecadal Oscillation. J. Mar. Syst. **133**: 77–87. doi:10.1016/j.jmarsys.2013.03.003.

García de Leániz, C., and Martínez, J.J. 1988. The Atlantic salmon in the rivers of Spain, with particular reference to Cantabria. *In* Atlantic salmon: planning for the future. *Edited by* D. Mills and D. Piggins. Croom Helm, London. pp. 179–209.

Golyandina, N., and Korobeynikov, A. 2014. Basic singular spectrum analysis and forecasting with R. Computational Statistics & Data Analysis, **71**: 934–954. doi:10.1016/j.csda.2013.04.009.

González-Taboada, F., and Anadón-Álvarez, R. 2011. Análisis de escenarios de cambio climático en Asturias. [Analysis of climate change scenarios in Asturias.] Available from https://www.asturias.es/medioambiente/publicaciones/ficheros/escenarios%20cambio%20climatico%20web%20af.pdf [accessed 17 July 2018].

Grimm, E.C. 1987. CONISS: A FORTRAN 77 program for stratigraphically constrained cluster analysis by the method of incremental sum of squares. Comput. Geosci. **13**(1): 13–35. doi:10.1016/0098-3004(87)90022-7.

Gullestad, P., Aglen, A., Bjordal, Å., Blom, G., Johansen, S., Krog, J., Misund, O.A., and Røttingen, I. 2014. Changing attitudes 1970–2012: evolution of the Norwegian management framework to prevent overfishing and to secure long-term sustainability. ICES J. Mar. Sci. **71**(2): 173–182. doi:10.1093/icesjms/fst094.

Hansen, L.P., and Jonsson, B. 1991. Evidence of a genetic component in seasonal return pattern of Atlantic salmon (*Salmo salar* L.). J. Fish Biol. **38**(2): 251–258. doi:10.1111/j.1095-8649.1991.tb03111.x.

Hari, R.E., Livingstone, D.M., Siber, R., Burkhardt-Holm, P., and Güttinger, H. 2006. Consequences of climatic change for water temperature and brown trout populations in Alpine rivers and streams. Glob. Change Biol. **12**(1): 10–26. doi:10.1111/j.1365-2486.2005.001051.x.

Harris, V., Edwards, M., and Olhede, S.C. 2014. Multidecadal Atlantic climate variability and its impact on marine pelagic communities. J. Mar. Syst. **133**: 55–69. doi:10.1016/j.jmarsys.2013.07.001.

Hátún, H., Payne, M.R., Beaugrand, G., Reid, P.C., Sandø, A.B., Drange, H., Hansen, B., Jacobsen, J.A., and Bloch, D. 2009. Large bio-geographical shifts in the north-eastern Atlantic Ocean: From the subpolar gyre, via plankton, to blue whiting and pilot whales. Prog. Oceanogr. **80**(3–4): 149–162. doi:10.1016/j.pocean.2009.03.001.

Haugland, M., Holst, J.C., Holm, M., and Hansen, L.P. 2006. Feeding of Atlantic salmon (*Salmo salar* L.) post-smolts in the Northeast Atlantic. ICES J. Mar. Sci. **63**(8): 1488–1500. doi:10.1016/j.icesjms.2006.06.004.

Haylock, M.R., Hofstra, N., Klein Tank, A.M.G., Klok, E.J., Jones, P.D., and New, M. 2008. A European daily high-resolution gridded dataset of surface temperature and precipitation. J. Geophys. Res. **113**(D20): 1–12. doi:10.1029/2008JD010201.

Holmes, E.E., Ward, E.J., and Scheuerell, M.D. 2018. MARSS: analysis of multivariate time-series using the MARSS package. R package version 3.10.10.

Horreo, J.L., Machado-Schiaffino, G., Ayllon, F., Griffiths, A.M., Bright, D., Stevens, J.R., and García-Vázquez, E. 2011*a*. Impact of climate change and human-mediated introgression on southern European Atlantic salmon populations. Glob. Change Biol. **17**(5): 1778–1787. doi:10.1111/j.1365-2486.2010.02350.x.

Horreo, J.L., Machado-Schiaffino, G., Griffiths, A.M., Bright, D., Stevens, J.R., and García-Vázquez, E. 2011*b*. Atlantic salmon at risk: apparent rapid declines in effective population size in southern European populations. Trans. Am. Fish. Soc. **140**(3): 605–610. doi:10.1080/00028487.2011.585574.

Huang, B., and National Center for Atmospheric Research Staff. (*Editors*). 2017. The Climate Data Guide: SST data: NOAA Extended Reconstruction SSTs, Version 4.

Hurrell, J., and National Center for Atmospheric Research Staff. (*Editors*). 2017. The Climate Data Guide: Hurrell North Atlantic Oscillation (NAO) Index (station-based).

Hurrell, J.W., Kushnir, Y., Ottersen, G., and Visbeck, M. 2003. The North Atlantic Oscillation: climatic significance and environmental impact. American Geophysical Union, Geophysical Monograph Series, Washington, D.C.

Husson, F., and Josse, J. 2017. missMDA: handling missing values with multivariate data analysis. R Package Version 1.11.

Husson, F., Josse, J., Lê, S., and Mazet, J. 2017. FactoMineR: multivariate exploratory data analysis and data mining. R Package Version 1.36.

Hvidsten, N.A., Diserud, O.H., Jensen, A.J., Jensås, J.G., Johnsen, B.O., and Ugedal, O. 2015. Water discharge affects Atlantic salmon *Salmo salar* smolt production: a 27 year study in the River Orkla, Norway. J. Fish Biol. **86**(1): 92–104. doi:10.1111/jfb.12542. PMID:25418585.

ICES. 2018. Report of the Working Group on North Atlantic Salmon (WGNAS), 4–13 April 2018, Woods Hole, Mass., USA. ICES CM 2018/ACOM: 21, 386 pp.

Jacobsen, J.A., and Hansen, L.P. 2001. Feeding habits of wild and escaped farmed Atlantic salmon, *Salmo salar* L., in the Northeast Atlantic. ICES J. Mar. Sci. **58**(4): 916–933. doi:10.1006/jmsc.2001.1084.

Jacobsen, J.A., Hansen, L.P., Bakkestuen, V., Halvorsen, R., Reddin, D.G., White, J., Maoiléidigh, N.Ó., Russell, I.C., Potter, E.C.E., Fowler, M., Smith, G.W., Mork, K.A., Isaksson, A., Oskarsson, S., Karlsson, L., and Pedersen, S. 2012. Distribution by origin and sea age of Atlantic salmon (*Salmo salar*) in the sea around the Faroe Islands based on analysis of historical tag recoveries. ICES J. Mar. Sci. **69**(9): 1598–1608. doi:10.1093/icesjms/fss115.

Johns, D. 2017. Monthly averaged data for *Calanus finmarchicus*, *Calanus helgolandicus*, Phytoplankton colour index, total euphausiids, total large copepods and total small copepods (44–65N, 55W–20E) 1950–2015 as recorded by the Continuous Plankton Recorder, Sir Alister Hardy Foundation for Ocean Science. Plymouth. doi:10.7487/2017.129.1.1054.

Jonsson, B., and Jonsson, N. 2004. Factors affecting marine production of Atlantic salmon (*Salmo salar*). Can. J. Fish. Aquat. Sci. **61**(12): 2369–2383. doi:10.1139/f04-215.

Jonsson, B., and Jonsson, N. 2009. A review of the likely effects of climate change on anadromous Atlantic salmon *Salmo salar* and brown trout *Salmo trutta*, with particular reference to water temperature and flow. J. Fish Biol. **75**(10): 2381–2447. doi:10.1111/j.1095-8649.2009.02380.x. PMID:20738500.

Jonsson, B., and Jonsson, N. 2011. Ecology of Atlantic salmon and brown trout: habitat as a template for life histories. Springer, Dordrecht, the Netherlands.

Jonsson, B., and Jonsson, N. 2017. Fecundity and water flow influence the dynamics of Atlantic salmon. Ecol. Freshw. Fish, **26**(3): 497–502. doi:10.1111/eff.12294.

Jonsson, B., Jonsson, N., and Finstad, A.G. 2013. Effects of temperature and food quality on age at maturity of ectotherms: an experimental test of Atlantic salmon. J. Anim. Ecol. **82**(1): 201–210. doi:10.1111/j.1365-2656.2012.02022.x. PMID:22905937.

Jonsson, B., Jonsson, N., and Albretsen, J. 2016. Environmental change influences the life history of salmon *Salmo salar* in the North Atlantic Ocean. J. Fish Biol. **88**(2): 618–637. doi:10.1111/jfb.12854. PMID:26725985.

Juggins, S. 2017. Rioja: analysis of quaternary science data. R Package Version 0.7-3.

Kendall, M. 1975. Multivariate analysis. Charles Griffin & Company, London.

Korobeynikov, A., Shlemov, A., Usevich, K., and Golyandina, N. 2016. Rssa: a collection of methods for singular spectrum analysis. R Package Version 0.14.

Lassalle, G., and Rochard, E. 2009. Impact of twenty-first century climate change

on diadromous fish spread over Europe, North Africa and the Middle East. Glob. Change Biol. **15**(5): 1072–1089. doi:10.1111/j.1365-2486.2008.01794.x.

Lear, W.H. 1980. Food of Atlantic salmon in the West Greenland–Labrador Sea area. Rapp. Proc.-Verb. Reun. Cons. Int. Explor. Mer, **176**: 55–59.

Legendre, P., Dallot, S., and Legendre, L. 1985. Succession of species within a community: chronological clustering, with applications to marine and freshwater zooplankton. Am. Nat. **125**(2): 257–288. doi:10.1086/284340.

Lenoir, J., Gégout, J.C., Marquet, P.A., de Ruffray, P., and Brisse, H. 2008. A significant upward shift in plant species optimum elevation during the 20th century. Science, **320**, 1768–1771.

Luczak, C., Beaugrand, G., Jaffré, M., and Lenoir, S. 2011. Climate change impact on Balearic shearwater through a trophic cascade. Biol. Lett. **7**(5): 702–705. doi:10.1098/rsbl.2011.0225. PMID:21508020.

MacKenzie, K.M., Palmer, M.R., Moore, A., Ibbotson, A.T., Beaumont, W.R.C., Poulter, D.J.S., and Trueman, C.N. 2011. Locations of marine animals revealed by carbon isotopes. Sci. Rep. **1**: 21. doi:10.1038/srep00021. PMID:22355540.

MacKenzie, K.M., Trueman, C.N., Palmer, M.R., Moore, A.J., Ibbotson, A.T., Beaumont, W.R.C., and Davidson, I.C. 2012. Stable isotopes reveal age-dependent trophic level and spatial segregation during adult marine feeding in populations of salmon. ICES J. Mar. Sci. **69**(9): 1637–1645. doi:10.1093/icesjms/fss074.

Mann, H.B. 1945. Nonparametric tests against trend. Econometrica, **13**(3): 245–259. doi:10.2307/1907187.

Mills, K.E., Pershing, A.J., Sheehan, T.F., and Mountain, D. 2013. Climate and ecosystem linkages explain widespread declines in North American Atlantic salmon populations. Glob. Change Biol. **19**(10): 3046–3061. doi:10.1111/gcb.12298.

Morice, C.P., Kennedy, J.J., Rayner, N.A., and Jones, P.D. 2012. Quantifying uncertainties in global and regional temperature change using an ensemble of observational estimates: The HadCRUT4 dataset. J. Geophys. Res. **117**(D8): D08101. doi:10.1029/2011JD017187.

Myneni, R.B., Keeling, C.D., Tucker, C.J., Asrar, G., and Nemani, R.R. 1997. Increased plant growth in the northern high latitudes from 1981 to 1991. Nature, **386**: 698–702. doi:10.1038/386698a0.

Nicola, G.G., Elvira, B., Jonsson, B., Ayllón, D., and Almodóvar, A. 2018. Local and global climatic drivers of Atlantic salmon decline in southern Europe. Fish. Res. **198**: 78–85. doi:10.1016/j.fishres.2017.10.012.

Nye, J.A., Baker, M.R., Bell, R., Kenny, A., Kilbourne, K.H., Friedland, K.D., Martino, E., Stachura, M.M., Van Houtan, K.S., and Wood, R. 2014. Ecosystem effects of the Atlantic Multidecadal Oscillation. J. Mar. Syst. **133**: 103–116. doi:10.1016/j.jmarsys.2013.02.006.

Olafsson, K., Einarsson, S.M., Gilbey, J., Pampoulie, C., Hreggvidsson, G.O., Hjorleifsdottir, S., and Gudjonsson, S. 2016. Origin of Atlantic salmon (*Salmo salar*) at sea in Icelandic waters. ICES J. Mar. Sci. **73**(6): 1525–1532. doi:10.1093/icesjms/fsv176.

Olden, J.D., and Poff, N.L. 2003. Redundancy and the choice of hydrologic indices for characterizing streamflow regimes. River Res. Appl. **19**(2): 101–121. doi:10.1002/rra.700.

Otero, J., Jensen, A.J., L'Abée-Lund, J.H., Stenseth, N.C., Storvik, G.O., and Vøllestad, L.A. 2011. Quantifying the ocean, freshwater and human effects on year-to-year variability of one-sea-winter Atlantic salmon angled in multiple Norwegian rivers. PLoS ONE, **6**: e24005. doi:10.1371/journal.pone.0024005. PMID:21897867.

Otero, J., L'Abée-Lund, J.H., Castro-Santos, T., Leonardsson, K., Storvik, G.O., Jonsson, B.,, et al. 2014. Basin-scale phenology and effects of climate variability on global timing of initial seaward migration of Atlantic salmon (*Salmo salar*). Glob. Change Biol. **20**(1): 61–75. doi:10.1111/gcb.12363.

Pauly, D. 1980. On the interrelationships between natural mortality, growth parameters, and mean environmental temperature in 175 fish stocks. ICES J. Mar. Sci. **39**(2): 175–192. doi:10.1093/icesjms/39.2.175.

Piou, C., and Prévost, E. 2013. Contrasting effects of climate change in continental vs. oceanic environments on population persistence and microevolution of Atlantic salmon. Glob. Change Biol. **19**(3): 711–723. doi:10.1111/gcb.12085.

Pyper, B.J., and Peterman, R.M. 1998. Comparison of methods to account for autocorrelation in correlation analyses of fish data. Can. J. Fish. Aquat. Sci. **55**(9): 2127–2140. doi:10.1139/f98-104.

R Core Team. 2017. R: a language and environment for statistical computing. v.3.3.3. R Foundation for Statistical Computing, Vienna, Austria.

Reddin, D.G., Hansen, L.P., Bakkestuen, V., Russell, I., White, J., Potter, E.C.E., Dempson, J.B., Sheehan, T.F., Maoiléidigh, N.Ó., Smith, G.W., Isaksson, A., Jacobsen, J.A., Fowler, M., Mork, K.A., and Amiro, P. 2012. Distribution and biological characteristics of Atlantic salmon (*Salmo salar*) at Greenland based on the analysis of historical tag recoveries. ICES J. Mar. Sci. **69**(9): 1589–1597. doi:10.1093/icesjms/fss087.

Reid, P.C., Borges, M., and Svenden, E. 2001. A regime shift in the North Sea circa 1988 linked to changes in the North Sea horse mackerel fishery. Fish. Res. **50**(1–2): 163–171. doi:10.1016/S0165-7836(00)00249-6.

Reid, P.C., Colebrook, J.M., Matthews, J.B.L., Aikend, J., and Continuous Plankton Recorder Team. 2003. The Continuous Plankton Recorder: concepts and history, from Plankton Indicator to undulating recorders. Prog. Oceanogr. **58**(2–4): 117–173. doi:10.1016/j.pocean.2003.08.002.

Renkawitz, M.D., Sheehan, T.F., Dixon, H.J., and Nygaard, R. 2015. Changing trophic structure and energy flow in the Northwest Atlantic: implications for Atlantic salmon feeding at West Greenland. Mar. Ecol. Prog. Ser. **538**: 197–211. doi:10.3354/meps11470.

Richter, B.D., Baumgartner, J.V., Powell, J., and Braun, D.P. 1996. A method for assessing hydrologic alteration within ecosystems. Conserv. Biol. **10**(4): 1163–1174. doi:10.1046/j.1523-1739.1996.10041163.x.

Rodionov, S. 2006. Use of prewhitening in climate regime shift detection. Geophys. Res. Lett. **33**(12): L12707. doi:10.1029/2006GL025904.

Russell, I.C., Aprahamian, M.W., Barry, J., Davidson, I.C., Fiske, P., Ibbotson, A.T., Kennedy, R.J., Maclean, J.C., Moore, A., Otero, J., Potter, E.C.E., and Todd, C.D. 2012. The influence of the freshwater environment and the biological characteristics of Atlantic salmon smolts on their subsequent marine survival. ICES J. Mar. Sci. **69**(9): 1563–1573. doi:10.1093/icesjms/fsr208.

Schewe, J., Heinke, J., Gerten, D., Haddeland, I., Arnell, N.W., Clark, D.B.,, et al. 2014. Multimodel assessment of water scarcity under climate change. Proc. Natl. Acad. Sci. U.S.A. **111**(9): 3245–3250. doi:10.1073/pnas.1222460110. PMID:24344289.

Schlesinger, M.E., and Ramankutty, N. 1994. An oscillation in the global climate system of period 65–70 years. Nature, **367**: 723–726. doi:10.1038/367723a0.

Sunday, J.M., Bates, A.E., and Dulvy, N.K. 2012. Thermal tolerance and the global redistribution of animals. Nat. Clim. Chang. **2**: 686–690. doi:10.1038/nclimate1539.

Sutton, R.T., and Hodson, D.L.R. 2005. Atlantic Ocean forcing of North American and European summer climate. Science, **309**(5731): 115–118. doi:10.1126/science.1109496. PMID:15994552.

The Nature Conservancy. 2009. Indicators of Hydrologic Alteration Version 7.1 User's Manual.

Urban, M.C. 2015. Accelerating extinction risk from climate change. Science, **348**(6234): 571–573. doi:10.1126/science.aaa4984. PMID:25931559.

Valiente, A.G., Beall, E., and García-Vázquez, E. 2010. Population genetics of south European Atlantic salmon under global change. Glob. Change Biol. **16**(1): 36–47. doi:10.1111/j.1365-2486.2009.01922.x.

Valiente, A.G., Beall, E., and García-Vázquez, E. 2011. Increasing regional temperatures associated with delays in Atlantic salmon sea-run timing at the southern edge of the European distribution. Trans. Am. Fish. Soc. **140**(2): 367–373. doi:10.1080/00028487.2011.557018.

Vøllestad, L.A., Hirst, D., L'Abée-Lund, J.H., Armstrong, J.D., MacLean, J.C., Youngson, A.F., and Stenseth, N.C. 2009. Divergent trends in anadromous salmonid populations in Norwegian and Scottish rivers. Proc. R. Soc. B Biol. Sci. **276**(1659): 1021–1027. doi:10.1098/rspb.2008.1600.

Webster, R. 1973. Automatic soil-boundary location from transect data. J. Int. Assoc. Math. Geol. **5**(1): 27–37. doi:10.1007/BF02114085.

Yue, S., Pilon, P., Phinney, B., and Cavadias, G. 2002. The influence of autocorrelation on the ability to detect trend in hydrological series. Hydrol. Process. **16**(9): 1807–1829. doi:10.1002/hyp.1095.

This article has been cited by:

1. Ana Almodóvar, Graciela G Nicola, Daniel Ayllón, Clive N Trueman, Ian Davidson, Richard Kennedy, Benigno Elvira. 2020. Stable isotopes suggest the location of marine feeding grounds of South European Atlantic salmon in Greenland. *ICES Journal of Marine Science* **77**:2, 593-603. [Crossref]
2. Francisco Nunes Godinho, Paulo Pinheiro. 2019. Occurrence of Atlantic salmon in the Douro River: Recent evidence. *Journal of Applied Ichthyology* **35**:6, 1300-1302. [Crossref]